Multidecadal Trends in Ozone Chemistry in the Baltimore-Washington Region

Sandra J. Roberts[1], Ross J. Salawitch[1,2,3], Glenn M. Wolfe[4], Margaret R. Marvin[1,5], Timothy P. Canty[2], Dale J. Allen[2], Dolly L. Hall-Quinlan[2], David J. Krask[6], Russell R. Dickerson[2]

1. Department of Chemistry and Biochemistry, University of Maryland, College Park, MD 20742, USA
2. Department of Atmospheric and Oceanic Science, University of Maryland, College Park, MD 20742, USA
3. Earth System Science Interdisciplinary Center, University of Maryland, College Park, MD 20742, USA
4. Atmospheric Chemistry and Dynamics Laboratory, NASA Goddard Space Flight Center, Greenbelt, MD 20771, USA
5. National Centre for Earth Observation, University of Edinburgh, Edinburgh, UK
6. Air Monitoring Program, Maryland Department of the Environment, Baltimore, MD 21230, USA

Correspondence to: Sandra J. Roberts (srobe@umd.edu)

Abstract

Over the past four decades, policy-led reductions in anthropogenic emissions have improved air quality over the Baltimore-Washington region (BWR). Most of the improvements in meeting the ozone air quality metrics (NAAQS) did not occur until the early 2000s despite large reductions in ozone precursors (NO_x, CO, and volatile organic compounds (VOCs)) in the prior decades. We use observations of ozone and ozone precursors from satellites, ground-based sites, and the 2011 DISCOVER-AQ aircraft campaign in Maryland to illustrate how ozone chemistry in the BWR evolved between 1972 and 2019. Analysis of weekday vs weekend probability of ozone exceedance indicates the BWR transitioned to the NO_x-limited regime by 2000-2003. A data-constrained box model agrees with this transition period and illustrates the key roles of reduced emissions of formaldehyde (HCHO), aromatics, and other VOCs since 1996, which

reduced the peak of ozone production at the time of the transition and likely prevented the BWR from experiencing worsening surface air quality as the region transitioned to NO_x-limited chemistry. Analysis of satellite observations of tropospheric column HCHO to NO_2 analyzed using a new approach for evaluation of chemical regimes derived from DISCOVER-AQ data also provide a consistent depiction of the timing of the transition period that we infer from ground-based observations and the box model. Finally, despite significant improvements in air quality over the past two decades, the BWR still has not met the EPA standard for surface ozone. With predominantly NOx-limited ozone chemistry over the BWR, continued decreases in emission of NOx will slow the rate of ozone production and help improve air quality. We highlight emissions of NO_2 from the diesel truck fleet as a worthwhile focus for future policy because emissions from this source appear to influence day-of-week variations in observed NO_2, with an accompanying effect on ozone.

Highlights

1. O3 in BWR had a nonlinear response to NOx reductions but are now sensitive to NOx
2. Diesel trucks in BWR are a major contributor to weekly trends in NOx and likely O3
3. VOC reductions had a major contribution to decreases in PO3 at Essex, MD until 2004
4. Both O3 chemical regimes were observed over BWR for HCHO/NO2 ratios between 1.2-2.2

Keywords: Ozone, NO_x, Air Quality, Box Model, OMI, VOC, F0AM, DISCOVER-AQ, air pollution

1. Introduction

Despite decades of decreased air pollutant emissions, the Baltimore-Washington Region (BWR) remains a nonattainment area under the United States' Environmental Protection Agency's (EPA) National Ambient Air Quality Standard (NAAQS) for tropospheric ozone (EPA Green Book, 2019). These health-based standards are necessary to ensure the health of the population; elevated ozone levels are linked to increased childhood asthma, hospitalizations, and premature death (Ryan et al., 1998; Mudway, 2000; Gryparis et al., 2004; Bell et al., 2006; Devlin et al., 2012; EPA, 2014). In recent years, progress has been made towards attaining EPA's 2015 NAAQS ozone standard of 70 ppbv ozone for the daily maximum 8-hour average in the BWR. Currently, the most polluted EPA-designated areas in this region are classified by the EPA as "marginal" nonattainment; prior to 2005, the region had been consistently classified as "severe" nonattainment (EPA Green Book, 2019). The poor air quality in the BWR stems both from local emission sources (vehicular and industrial) and transport of pollutants from upwind sources (Hains et al., 2008; Walsh et al., 2008; He et al., 2013a; Brent et al., 2015; Goldberg et al., 2015; Jaffe et al., 2018). Science-informed policies aimed to decrease pollutants from these emission sources have helped the BWR become closer to attainment of the NAAQS for tropospheric ozone (Frost et al., 2006; Godowitch et al., 2008; Pegues et al., 2012; Aburn et al., 2015).

Of the six criteria air pollutants regulated by the EPA, ozone is among the most difficult to control due to the complex, nonlinear chemistry of its production (Chameides & Walker, 1973; Sillman et al., 1990; Monks, 2005). As a secondary pollutant, ozone is not emitted;

instead, ozone is produced in a series of photochemical reactions between other directly emitted pollutants. These ozone precursors, which include volatile organic compounds (VOCs), carbon monoxide (CO), and oxides of nitrogen (NO_x = NO+NO_2), react to produce ozone. Ozone production has a nonlinear relationship with its precursors, so it is necessary to know the concentrations of these species and understand the chemistry behind ozone production to effectively reduce concentrations (Crutzen, 1971, 1973; Sillman et al., 1990; Jacob et al., 1993; Pusede & Cohen, 2012; Pusede et al., 2015; Simon et al., 2015; Nussbaumer & Cohen, 2020). Recent work also suggests quantifying background ozone, or ozone that is not produced from anthropogenic sources emitted within the United States, has become increasingly important as background ozone is a large contributor to observed ozone concentrations (Shen & Mickley, 2017; Shen et al., 2017; Jaffe et al., 2018; Parrish & Ennis, 2019).

Ozone is produced in a catalytic cycle in the presence of sunlight. The cycle is initialized with the oxidation of CO or a VOC by the hydroxyl radical (OH) and then, in the presence of oxygen, peroxy radicals (RO_x = HO_2 + RO_2) are formed (Crutzen, 1971; Levy, 1972; Pratapas & Calcagni, 1983; Lin et al., 1988; McConnell & Schwab, 1990; Korsog & Wolff, 1991; Jacob, 2009). These radicals then oxidize NO, producing NO_2, which in turn is photolyzed into NO and $O(^3P)$. Finally, $O(^3P)$ reacts with molecular oxygen (O_2) to produce ozone. The rate-limiting step in this cycle is the reaction of NO with the peroxy radicals, thus the ozone production rate (PO_3) is calculated using

$$PO_3 = [NO](k_1[HO_2] + \sum k_i[RO_2]_i) \qquad \textbf{Equation 1}$$

where k_1 is the rate constant of the reaction of NO with HO_2 and k_i is the rate constant of the reaction of NO with a given alkylperoxy radical.

The nonlinear relationship between ozone and its precursors results in two distinctive regimes of ozone production rates. The amount of ozone produced initially rises with increased NO_x emissions, but as NO_x concentrations continue to increase, the radical terminating reaction of $OH+NO_2$ competes with the oxidation of VOCs by OH, producing fewer peroxy radicals and suppressing the production of ozone. The first, in which PO_3 rises with increasing NO_x concentrations and is highly sensitive to NO_x concentrations, is called the NO_x-limited regime. The second regime is referred to as the NO_x-saturated regime, where high NO_x concentrations suppress ozone production and the chemistry is more sensitive to changes in VOC concentrations (Sillman et al., 1990; Milford et al., 1994; Sillman, 1995; Kleinman et al., 1997; Pusede et al., 2015).

To implement proper ozone control strategies, the regional sensitivity of ozone chemistry must be understood. NO_x reductions will reduce ozone if the ozone chemistry in a given region is NO_x-limited (Frost et al., 2006; Simon et al., 2015). If a city begins in the NO_x-saturated regime, strategies focused only on reductions in the emission of NO_x will initially lead to increases in ozone concentrations in the immediate urban area (Heuss et al., 2003; Murphy et al., 2007; Pusede et al., 2015; Simon et al., 2015; Nussbaumer & Cohen, 2020). In this case, VOC reductions would be the most useful strategy to immediately mitigate ozone pollution in the urban core. However, peak ozone production often occurs in NO_x-limited regions downwind of major urban areas, so region-wide NO_x reductions are always beneficial to reduce the population exposure to harmful concentrations of ozone (Sillman et al., 1990; Jin et al., 2020). In other words, a NO_x-saturated air parcel from an urban region will become NO_x-limited as the parcel travels to downwind rural and forested areas.

Since 1972, the abundances of anthropogenic VOCs, CO, and NO_x have decreased in the BWR as a response to policies implemented to reduce ozone and other criteria pollutants (**Figure 1**). Early efforts on ozone control in the BWR were focused on reducing VOCs and CO (Lebron, 1975; Wolff, 1993; Jacob, 2009). These VOC control strategies were not as effective as models predicted in reducing ozone exceedances in the BWR because biogenic VOC emissions were not represented well(Lebron, 1975; Korsog & Wolff, 1991; Jacob, 2009). Studies have since shown that VOC chemistry in the eastern United States is often dominated by isoprene, a highly reactive VOC (Trainer et al., 1987; Chameides et al., 1988). Since the update to the Clean Air Act in 1990, control strategies have been aimed at reducing emissions of NO_x from vehicles and stationary sources (Frost et al., 2006). Despite dramatic reductions in the atmospheric abundance of NO_2, the Baltimore-Washington region maintained a high number of yearly ozone exceedances, with the maximum 8-hour ozone observed in the BWR on hot days ($T \geq 31.7°C$) decreasing by a little over 10 ppbv between 1980 and 2004 (**Figure 1**). This slow decrease in ozone resulted in the BWR remaining classified by the EPA as a severe nonattainment zone for ozone (EPA Green Book, 2019). Further reductions in NO_x occurred after the 2003 State Implementation Plan (SIP), which aggressively drove down emissions of NO_x from power plants in both Maryland and upwind states (Frost et al., 2006; Bloomer et al., 2009), resulting in ozone reductions that were underestimated by air quality models at the time (Gilliland et al., 2008). The highest concentrations of ozone declined rapidly between 2002 and 2019, with a decrease of nearly 30 ppbv in maximum 8-hour ozone concentration on hot days in the BWR (**Figure 1**).

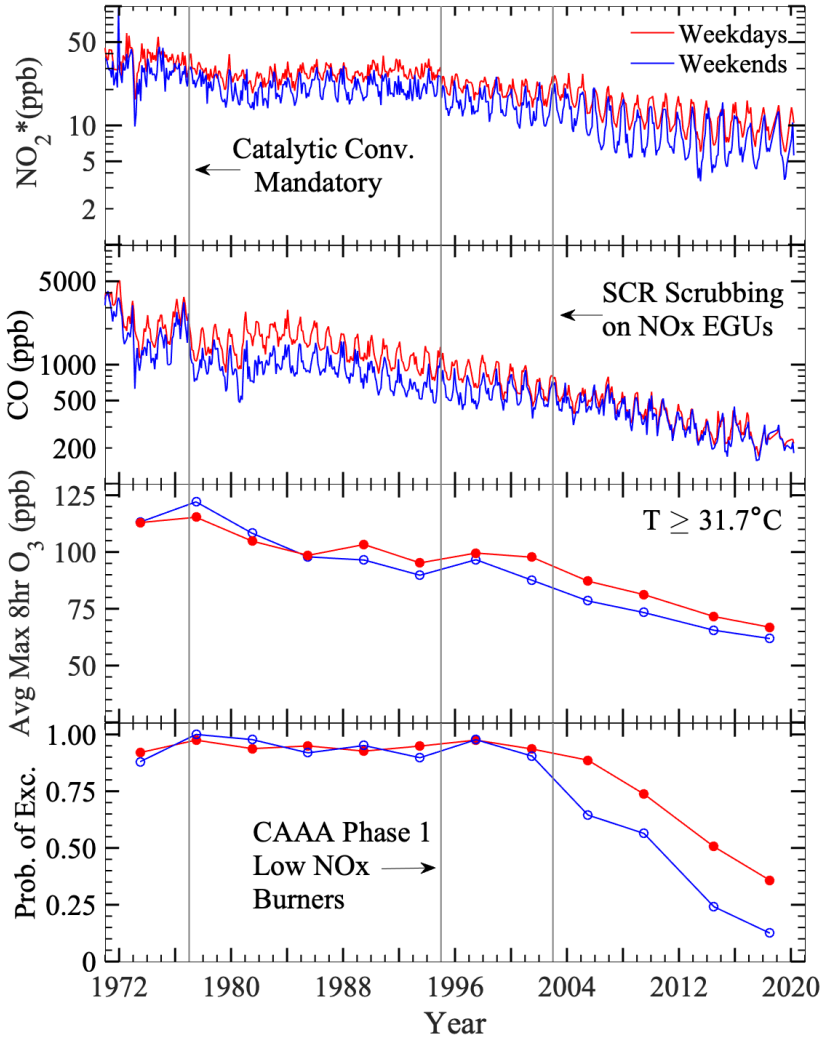

Figure 1 Monthly mean measured NO_2 (NO_2*,top) and CO (2nd panel) mixing ratios for the BWR, separated by weekdays (red) and weekends (blue). Four-year averaged region-wide maximum 8-hour ozone (3rd panel) and probability exceedance (bottom panel) for days T ≥ 31.7°C (89°F) separated by weekdays and weekends over the period of 1972-2019. The dates of major policy implementations affecting NO_x and/or CO emissions are noted by gray lines.

The definition of the transition between the NO_x-limited and the NO_x-saturated regimes is not agreed upon in the literature. Some authors focus on a chemically-relevant transition, in which NO_x and VOCs have equal contribution to PO_3. Examples of such distinctions would be the ratio of H_2O_2/HNO_3 where values less than 0.35 indicate NO_x-limited chemistry (Milford et

al., 1994; Jacob et al., 1995) or using the ratio of L_N to Q (L_N/Q) where L_N is the radical termination due to NO_2+OH and Q is the total radical loss where ratios of less than 0.5 indicate NO_x-limited chemistry (Kleinman et al., 1997; Kleinman, 2005; Mao et al., 2010; Ren et al., 2013). The satellite-based approach to measuring ozone production sensitivity uses the relationship between the photochemically modeled L_N/Q ratio and the satellite-observed tropospheric column ratio of HCHO/NO_2 to determine the range of ratios indicative of NO_x-saturated or NO_x-limited chemistry. For example, HCHO/NO_2 ratios of less than one indicate NO_x-saturated chemistry and ratio values greater than two indicate NO_x-limited chemistry (Martin et al., 2004; Kaynak et al., 2009; Duncan et al., 2010). More recently, a policy-relevant transition has been used, in which the transition is defined at the peak of ozone production (Pusede & Cohen, 2012; Schroeder et al., 2017; Jin et al., 2020; Nussbaumer & Cohen, 2020). Pusede and Cohen (2012) use the probability of ozone exceedance (PoE) as a proxy for ozone production and defines NO_x-limited chemistry as when NO_2 and PoE have a positive correlation. In Schroeder et al. (2017), the transition value of the ozone sensitivity indicator of LRO_x/LNO_x is re-evaluated to indicate the peak of the ozone production curve. Defining the transition at the peak of ozone production helps to indicate to policy makers when a region will begin to see a decline in ozone production with reduction in NO_x concentrations. The policy-relevant transition point occurs at higher levels of NO_x, this indicates that the benefit of decreased NO_x emissions on PO_3 occurs prior to the chemically-relevant transition. In this paper, we focus on the policy-relevant transition, in which the dependence of ozone production on NO_2 is used as an indicator for ozone production regime and the transition between the regimes occurs at the peak of the ozone production curve.

Evaluating the difference in ozone chemistry between weekends and weekdays is a useful method of determining where a city lies on the ozone production curve (Lebron, 1975; Marr & Harley, 2002; Heuss et al., 2003; Murphy et al., 2007; Blanchard et al., 2008; Jin et al., 2020; Nussbaumer & Cohen, 2020). Due to differences in anthropogenic emissions, the concentration of NO_x is typically lower on weekends than on weekdays (Heuss et al., 2003; Gao, 2007). The longer lifetime of CO compared to NO_x and the dominance of biogenic emissions over anthropogenic emission of VOCs for the BWR means most of the weekend/weekday difference in ozone photochemistry is driven by NO_x. With this knowledge and the observed concentration of ozone on weekends and weekdays, there are two separate points to compare on the ozone production curve and infer the chemical regime for ozone production. Furthermore, the decreased anthropogenic emissions on weekends may give insight into the sectors that are most affecting the enhanced weekday concentration of ozone precursors. This distinction will aid policy makers in determining which emission sectors should be regulated to bring a region into compliance with the EPA NAAQS.

This paper details the change in ozone chemistry in the BWR between 1972-2019 using ground-based data, satellite observations, and box model simulations. Our focus is on June, July, and August because historically most violations of the NAAQS for surface ozone in the BWR occur during these three months. Long-term observations of ozone, CO, VOCs and NO_2 from EPA Air Quality System (AQS) sites across the BWR are used to determine how the ozone exceedance probability of an ozone exceedance changed as a function of measured NO_2 over this 48-year period. A 0-dimensional photochemical box model is implemented to identify the reductions in measured ozone precursor species that were most successful in decreasing ozone

production rates between 1996-2016 at a site near downtown Baltimore (Essex, MD) with a long-term record of speciated VOC measurements. The ratio of tropospheric column HCHO to NO_2 that indicates the transition from NO_x-saturated to NO_x-limited chemistry is then reassessed to represent the regional chemical conditions in the BWR using data from the 2011 DISCOVER-AQ campaign in Maryland. This reassessed ratio is applied to evaluate trends in ozone chemistry over the BWR with observed tropospheric column ratios of $HCHO/NO_2$ by satellites between 1996-2019. The results of these analyses reveal that early reductions in anthropogenic emissions of VOCs were the primary contributor to the improvement in ozone air quality at an urban site in the BWR. Furthermore, NO_x-limited ozone chemistry became the dominant regime of ozone production in the BWR in the early 2000s. Thus, continued decreases in the emission of NOx will aide in further improvement of surface ozone in the BWR.

2. Approach

2.1 Ground-Based Observations

Ground-based monitors, part of the EPA AQS monitoring network in Maryland, Washington, D.C., and northern Virginia are used in this analysis (**Figure 2**). This ground-based measurement network for criteria air pollutants such as CO, NO_2, and O_3, provides a record of air quality observations since 1972. The ground-based data used in this analysis were acquired from the EPA, and data from 1980-2019 are currently available through the EPA Data Mart (https://aqs.epa.gov/aqsweb/airdata/download_files.html). Hourly VOC data have been reported from Essex, Maryland through the Photochemical Assessment Monitoring Station (PAMS) program of the EPA since 1996 (EPA, 1996). Meteorological observations of

temperature, humidity, and pressure used in this analysis are from the Baltimore Washington International Airport (BWI), which is about 20 km from the Essex site.

Chemiluminescence was used to measure NO and NO_2 at the ground-based NO_x monitoring site in this analysis. This method for measuring NO_2 has well-known interferences from other reactive nitrogen species (e.g.: PAN, HNO_3, $RONO_2$) , as NO_2 must first be reduced to NO through a heated molybdenum catalyst (Winer et al., 1974; Grosjean & Harrison, 1985;

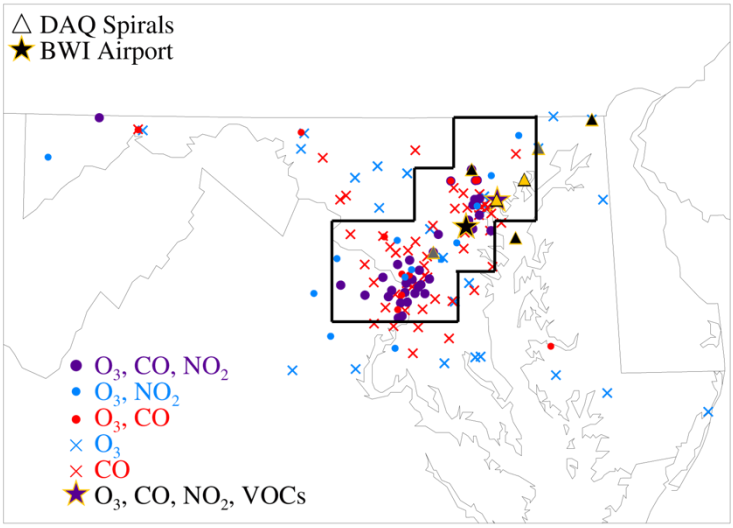

Figure 2 The location of the ground-based monitoring sites used in this analysis. The symbols represent any ground-based monitor that has recorded data between 1970-2019. The circles represent monitoring sites that recorded 2 or more species (purple-O_3, CO, and NO_2*, blue- O_3 and NO_2*, red- O_3, CO). Symbols marked by an X represent locations that only recorded one species. The star symbol denotes the PAMS-VOC site at Essex, MD, which records O_3, CO, NO_2*, and VOCs. The triangles are the locations of the spirals during the 2011 DAQ campaign and the color of the triangle represents the number of NO_x-suppressed spirals (gray- 0, black- 1, yellow- >1). The black boundary box represents the L3 satellite grid cells for the Baltimore-Washington Metropolitan area.

Fehsenfeld et al., 1990; Dunlea et al., 2007; Horowitz et al., 2007; Dickerson et al., 2019). The catalyst reduction reaction is known to reduce other reactive nitrogen species in addition to NO_2, resulting in artificially enhanced values of NO_2. In this paper, the measured NO_2

concentration will be referred to as NO_2*. For the analysis with the box model, the adjusted NO_2 concentration is approximated using

$$NO_{2,adjusted} = \frac{NO_2^*}{0.55(NO_2^* + NO_z)} \quad \textbf{Equation 2}$$

Where reactive nitrogen (NO_z) and NO_2* are based on measurements of all reactive nitrogen species (with NO_z represented by the sum of PAN and PAN-like compounds, alkyl nitrates, and HNO_3) during the 2011 DISCOVER Air Quality (DAQ) campaign in Maryland and adjusting for a known interference effect (Dunlea et al., 2007) that varies for time of day based on DAQ observations for NO_2 and NO_z.

2.2 Probability of Ozone Exceedance and Regional Maximum 8-hour Ozone Calculations

The chemical regime for ozone production was inferred using the probability of ozone exceedance in the BWR. Hourly ozone data from the local ground-based network in the BWR were used to calculate the daily maximum 8-hour average ozone for each ozone-monitoring site. Using the 2015 EPA NAAQS standard of 70 ppbv for 8-hour average ozone, a day was classified as an exceedance if any monitor had a maximum 8-hour average ozone concentration at or above 71 ppbv. The probability of ozone exceedance was determined for 4-year time bins over three temperature regimes. As in Pusede and Cohen (2012), temperature is used as a proxy for VOC reactivity (VOCR) (Pusede & Cohen, 2012; Pusede et al., 2015; Nussbaumer & Cohen, 2021). Of course, a number of other factors that affect surface ozone, such as rate constants and the emission of NO_x from power plants and vehicles, also vary as a function of temperature. Here, three regimes for maximum daily temperature were used: hot (T ≥ 31.7°C (89°F)), warm (28.9°C (84°F) ≤ T < 31.7°C), and moderate (26.1°C (79°F) ≤ T < 28.9°C). The

probability of ozone exceedance was then calculated as the number of exceedance days in a given temperature regime divided by the total number of days for each temperature regime. Regional maximum 8-hour ozone was calculated as the average of the highest 8-hour ozone concentration in the BWR for days within each temperature regime. These calculations were completed for both weekdays and weekends and plotted against the daily average 10 am-2pm observation of NO_2* (directly measured concentration of NO_2). This four hour time range is used to obtain mid-day average NO_2* because diurnal variations in NO_2, driven by the solar zenith angle dependence of the NO_2 photolysis frequency, are small (typically less than 10% according to our calculations) during these hours for clear sky, summer conditions.

2.3 Box model PO_3 calculation for year bins

A 0-D photochemical box model, Framework for 0-D Atmospheric Modeling (F0AM), was used to simulate atmospheric chemistry spanning 1996-2019 in 4-year time bins (Wolfe et al., 2016). The majority of ozone exceedances occur on hot days in the BWR; accordingly, the box model was constrained to measurements from hot days ($T \geq 31.7°C$) to represent days most conducive to ozone formation. The median hourly measurements of CO and O_3 from ground-based sites in the BWR and VOC data from the PAMS station in Essex, MD were used to constrain the model. Meteorological input for the model included temperature, pressure, and humidity data from BWI for days with a maximum temperature above 31.7°C. The NO_2 photolysis frequency was constrained in the model using radiometer measurements below 500 m during the 2011 DAQ campaign in Maryland. The model was run to steady state (72 hours) and all species are assigned a first-order physical loss rate coefficient of 1 day.

The impact of VOC and CO reductions on ozone production rate (PO_3) was evaluated within the CB6r2 chemical mechanism within F0AM (Whitten et al., 2010; Yarwood et al., 2012; Hildebrandt-Ruiz & Yarwood, 2013). Base case model runs were completed by constraining the model to the appropriate 4-year time bin concentrations of CO and O_3, and VOC concentrations. Curves for PO_3 were calculated by modeling each time bin for a range of NO_2 concentrations (1-20 ppbv) (**Figure 5**).

To determine how the reduction of each measured ozone precursor species influenced the decline in PO_3 between each consecutive time bin (e.g., 1996-1999 to 2000-2003), one species was analyzed at a time. To minimize the effects of nonlinearity, small perturbations were made for individual species. For example, a model run was completed with all species held at 1996-1999 concentrations and one species perturbed to its 2000-2003 concentration. The resulting difference in PO_3 between the base 1996-1999 run and the perturbed run was calculated at the 2000-2003 average NO_2 concentration and the difference in PO_3 was attributed to the perturbed species. This method was repeated for each following consecutive time bin (e.g., analyte species now at 2004-2007 concentrations with all other species held at 2000-2003 concentrations). The overall impact of each species on reducing the PO_3 between the first available complete bin (1996-1999) and the final complete time bin (2012-2015) was determined by summing the differences between the perturbed run and the base run. This set of calculations was conducted only through the 2012-2015 time bin because of the reduced frequency of aldehyde measurements beginning in 2016.

2.4 Ozone production regime calculation

Data from the 2011 Maryland DAQ were analyzed to evaluate metrics used to determine the ozone production regime. The DAQ campaign took place over and downwind of the Baltimore-Washington corridor in July 2011, the region's hottest July on record. During this campaign, NASA's P3-B flew 14 flights over a repeated flight path measuring the concentration of gaseous and particulate pollution over the region (NASA/LARC/SD/ASDC, 2014). These flights included several spirals over the Chesapeake Bay and 6 ground sites, the measurements from these spirals are used in this analysis to compare to satellite observations. The F0AM model with CB6r2 chemistry (Yarwood et al., 2012; Ruiz & Yarwood, 2013) was constrained using CO, O_3, NO_2, HNO_3, HCHO, isoprene, monoterpenes, acetaldehyde, acetone, methanol, methyl vinyl ketone, methacrolein, toluene, and xylenes measured by instruments on the NASA P3-8 during the campaign in July 2011. The model output was used to calculate the slope of PO_3 as a function of NO_2 ($\partial PO_3/\partial NO_2$) by constraining the model to a 0.25 ppbv NO_2 increment surrounding the measured value of NO_2. A measurement was categorized NO_x-limited if $\partial PO_3/\partial NO_2$ was positive and NO_x-saturated if $\partial PO_3/\partial NO_2$ was negative. The resulting $\partial PO_3/\partial NO_2$ was then compared to the ratios of tropospheric column $HCHO/NO_2$ and *in situ* $HCHO/NO_2$ calculated from the DAQ data (**Figure 6**).

The tropospheric column HCHO and NO_2 were calculated separately by integrating the measured species from the lowest to the topmost measurement in each spiral. To calculate tropospheric column, the highest point was extrapolated to the tropopause (200 hPa) and the bottommost mixing ratio was extrapolated to the surface (1013 hPa) by assuming a constant volume mixing ratio as a function of altitude between 200 hPa and the highest altitude as well as between the lowest altitude data and 1013 hPa (Flynn et al., 2014; Schroeder et al., 2017).

The ratio of column HCHO to column NO_2, denoted the tropospheric column ratio HCHO/NO_2, was then calculated and compared to the median $\partial PO_3/\partial NO_2$ within the boundary layer (altitude < 500 m). The ratio for *in situ* observations of HCHO and NO_2 within the boundary layer was also plotted against instantaneous values of model-calculated $\partial PO_3/\partial NO_2$. Both panels of the plot were colored by the time of day when the measurements were observed.

2.5 Satellite Ratio Calculations

The ozone production regime was also evaluated using satellite observations of tropospheric column abundances of HCHO and NO_2 measured with five satellite instruments. Satellite observations during a morning overpass time are available from the GOME (1996-2002) (Bednarz, 1995; Burrows et al., 1999; Boersma et al., 2004), SCIAMACHY (2003-2011) (Bovensmann et al., 1999; Boersma et al., 2004), GOME-2A (2007-present), and GOME-2B (2013-present) instruments (Callies et al., 2000; Boersma et al., 2004; Munro et al., 2016). Observations from an afternoon overpass time are available from OMI (2005-present) (Levelt et al., 2006a, 2006b; Boersma et al., 2011). The ratio of tropospheric column HCHO/NO_2 was used as an indicator of ozone production regime.

For each instrument, June-August (JJA) means of tropospheric column HCHO and NO_2 were calculated using available monthly-average L3 (gridded) satellite data. Time series of the HCHO/NO_2 ratios were constructed using grid cells over the Baltimore-Washington Metropolitan region (**Figure 2**) from the monthly satellite data. For consistency with the other instruments, the OMI measurements (OMI,obs) were adjusted to approximate a morning overpass time (OMI,adj) using

$$\left(\frac{HCHO}{NO_2}\right)_{OMI,adj} = 0.69\left(\frac{HCHO}{NO_2}\right)_{OMI,obs} + 0.08, \quad \textbf{Equation 3}$$

where the slope and the intercept were calculated from the diurnal variation of tropospheric column HCHO and NO_2 in the output of a Comprehensive Air Quality Models with extensions (CAMx) run for July 2011 over Maryland (Goldberg et al., 2016). The output from the CAMx run was from the 'Beta' model simulation (Goldberg et al., 2016), which has updates to both model chemistry and emissions. Tropospheric column ratios of HCHO and NO_2 were calculated with model output by applying the averaging kernels from GOME-2A data for morning columns and from OMI data for afternoon columns. The adjustment applied to OMI satellite data was calculated from the line of best fit for the plot of morning vs afternoon tropospheric column HCHO/NO_2. The resulting tropospheric column HCHO/NO_2 for all satellites were plotted as a time series to show how this ratio has changed over the Baltimore-Washington Metropolitan Region (**Figure 7**).

3. Results and Discussion

3.1 Inferring Transition to NO_x-limited Regime using Ground-Based Measurements

Changes in traffic and work patterns on the weekend relative to weekday account for the lower emissions of NO_x on weekends. This day-of-week effect occurs in the BWR with median, measured weekend NO_2* typically 20-40% lower than weekday NO_2* (**Figure 3a, d**). The observed decrease in NO_2 on the weekends can be used in conjunction with changes in observed ozone as an indicator of ozone production regime (Lebron, 1975; Marr & Harley, 2002; Heuss et al., 2003; Murphy et al., 2007; Blanchard et al., 2008; Pusede & Cohen, 2012).

Here, we examine the factors that influence the observed day-of-week change in NO_2* in the BWR and use the differences in weekend/weekday ozone exceedances to deduce when the BWR transitioned to primarily NO_x-limited chemistry.

The two sectors that dominate NO_x emissions in the BWR, mobile sources and electricity generating units (EGUs), both have a day-of-week variation in emissions. On two highly-traveled roads in the BWR (Interstate-95 and DC-295), traffic on the weekend shows a different daily cycle than during weekdays and is between 10-25% lower for passenger cars and 35-60% lower

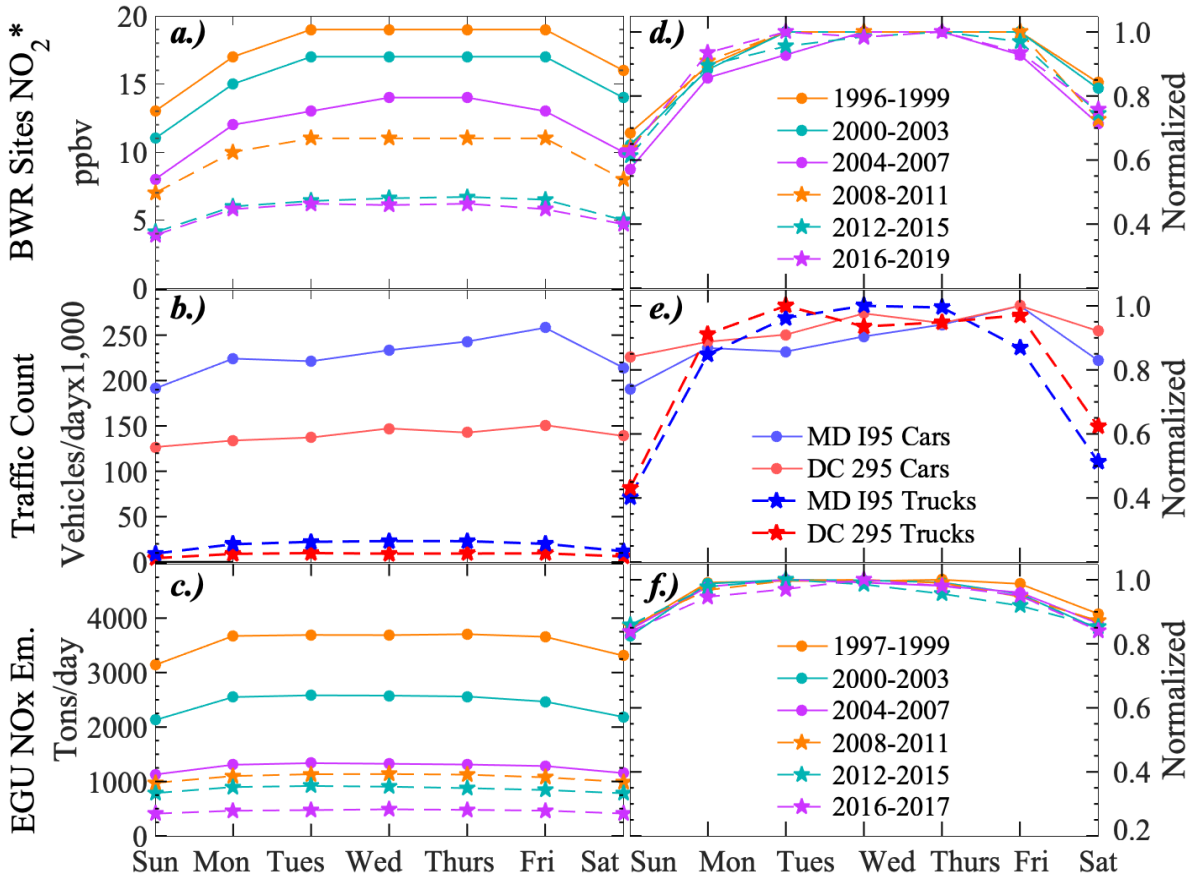

Figure 3 The median values of the June-July-August weekly trends of a. NO_2* measured at AQS sites in the BWR broken into 6 time bins, b. Vehicle traffic counts (2016-2017) separated by road (Interstate-95 and DC295) and vehicle type (passenger cars and trucks), and c. Continuous Emissions Monitoring System data of NO_x emissions from electrical generating units (EGU) from MD, OH, PA, VA, and WV divided into 6 time bins. Panels d-f show the day-of-week trend normalized to the maximum weekly value in each respective bin

for diesel trucks (**Figure 3b, e**). Diesel trucks emit about 8-10 times more NO_x per mile travelled than gasoline vehicles, which are primarily passenger cars and trucks (W. Kirchstetter et al., 1999; Ban-Weiss et al., 2008; Dallmann & Harley, 2010; McDonald et al., 2012). Consequently, diesel trucks are assumed to dominate the emission in NO_x in areas with > ~10% truck traffic, which is observed in the Baltimore-Washington corridor on weekdays (Hall et al., 2020).

While traffic patterns are often cited as the driving factor in the day of week variations in observed NO_2, EGUs also have decreased output and emissions on the weekend in the BWR, with emissions decreasing by about 15% on weekends when compared to week days (**Figure 3c,f**) (Pun et al., 2003; Kaynak et al., 2009). Model output analyzing the 10 worst air quality days in Edgewood, MD during July 2011 indicates that EGU emissions from Maryland and upwind states contribute roughly half as much to ozone as traffic emissions from Maryland and upwind states (Goldberg et al., 2016). Field experiments in recent years indicate that summer NO_x emissions from vehicles were overestimated by about 50% during the ozone season in the 2011 NEI inventory that is often used to drive air quality models (McDonald et al., 2013; Anderson et al., 2014; Canty et al., 2015; Travis et al., 2016; Ring et al., 2018; Hembeck et al., 2019). Vehicular emissions generally decrease on hot days while EGU emissions increase (He et al., 2013a; Hall et al., 2020). When a 50% reduction is applied to mobile emissions, EGU emissions become relatively more important on bad air quality days (Goldberg et al., 2016). Both day of week variations in both EGU and vehicle traffic can contribute to the overall decrease in NO_x over the BWR on weekends (**Figure 3**). However, day of week variations in NO_2* most closely correlate with variations in diesel truck traffic counts, with both diesel and NO_2* having the

lowest observations on Sundays. This correlation suggests that diesel truck emissions are an important contributor to observed changes in ozone exceedances in the BWR.

The probability of ozone exceedance was calculated separately for weekdays and weekends over 48 years. The data were separated into 12 time-bins; each time bin represents four years with the exception of the last bin, which covers only two years. The probability of

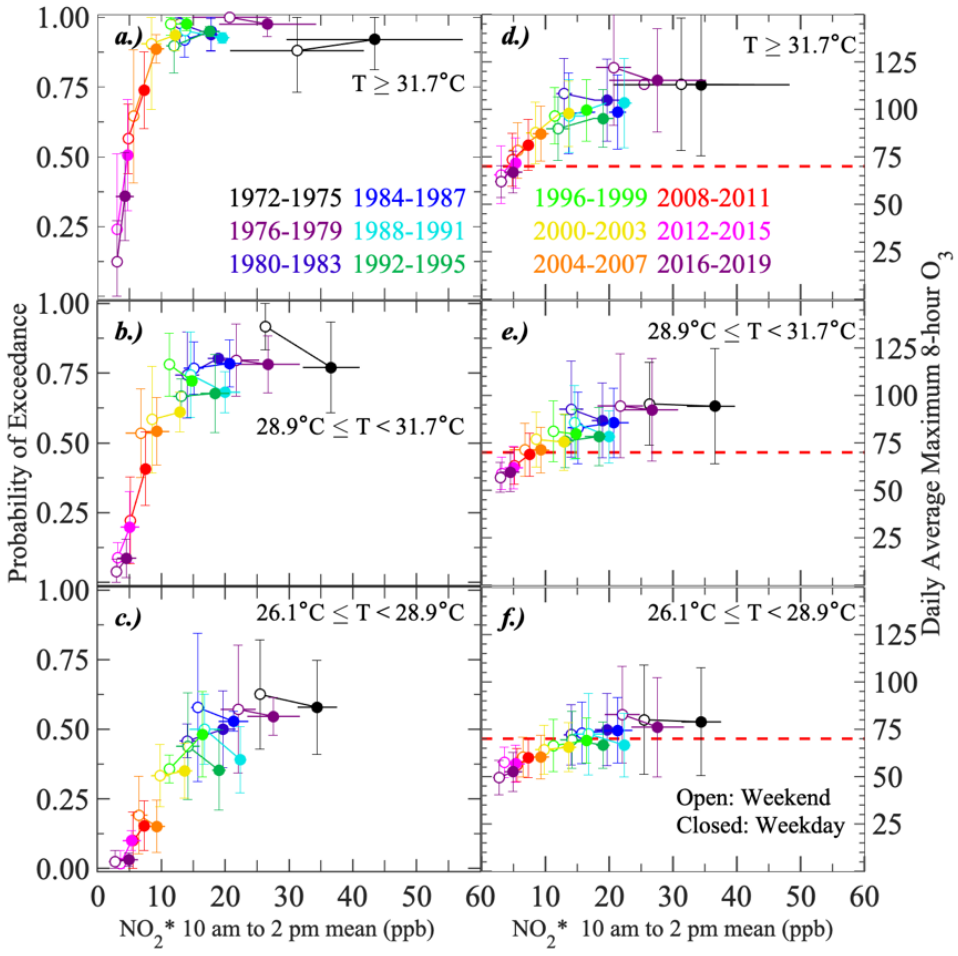

Figure 4 Four-year average probability of ozone exceedance (a,b,c) and region-wide maximum 8-hour ozone (d,e,f) for weekdays (closed circles) and weekends (open) plotted against average 10 am- 2pm NO_2*. Data are separated into 3 temperature regimes: a,d. Hot (T ≥ 31.7°C), b,e. Warm (28.9°C ≤ T < 31.7°C), and c,f. Moderate (26.1°C ≤ T < 28.9°C). Error bars represent uncertainty (1σ) in probability of exceedance, 8-hr average ozone, and NO_2* concentration. The red dashed line (d,e,f) represents the current 8-hour ozone standard (70 ppbv).

exceedance is further broken down into three temperature regimes: hot, warm, and moderate. These temperature regimes were selected to have a similar number of days in a year, with an average of 37, 40, and 39 days per year representing the hot, warm, and moderate temperature bins, respectively. The PoE is plotted as a function of daytime (10 am – 2 pm EST) NO_2* concentration in **Figure 4**. The response of PoE to changes in NO_2* on weekdays and weekends in each respective time bin is used as an indicator of the ozone production regime for the BWR.

As the probability of ozone exceedances has decreased in the BWR over the past 14 years, the weekend and weekday probability of exceedance on hot days has diverged (**Figure 4a**). For the first 28 years, on hot days, NO_2* decreased by 26 ppbv on weekdays and 19 ppbv on weekends. Despite the dramatic reduction in NO_2* in this time period, the probability of ozone exceedance remained near unity over the period and the maximum 8-hour ozone in the BWR on hot days decreased slowly. Between the 2000-2003 time bin and the final time bin (2016-2019), NO_2* on weekdays decreased by another 6 ppbv resulting in a decrease in the probability of ozone exceedance of 43%. Weekend air quality improved even more between these same two time periods; NO_2* decreased by 5 ppbv while the probability of ozone exceedance decreased by 67%. From the 2000-2003 time bin until the 2016-2019 time bin, the probability of exceedance became highly responsive to weekend decreases in NO_2*, indicating that the Baltimore-Washington region was within the NO_x-limited regime.

For the majority of hot days, PoE remained near unity, masking the trends in ozone chemistry through the 2000-2003 time bin. Regional maximum 8-hour ozone was used to provide further insight to the ozone chemistry in the BWR. When comparing the response of 8-

hour ozone to the change in NO_2* concentrations between weekday and weekend for each time bin, there are three distinct chemical groups. Between 1972-1988, 8-hour ozone either increased or remained the same on the weekends, indicating ozone chemistry that is NO_x-suppressed. From 1988-2000, 8-hour ozone and NO_2* decreased at a 1:1 ratio between weekday and weekend observations in each time bin, suggesting ozone chemistry was weakly NO_x-limited. Since 2000, a 1 ppbv decrease in NO_2* concentration on the weekend yields an average reduction in 8-hour ozone concentration between 2.5-4.1 ppbv, which demonstrates ozone chemistry has been highly NO_x-limited on hot days ($T \geq 31.7$°C) in the BWR since 2000. The probability of ozone exceedance has also fallen rapidly in the warm temperature regime, but the difference between weekend and weekday differs from what is observed on hot days. On warm weekdays, the probability of exceedance has decreased from 74% in the 1972-1975 time bin to 17% in the 2016-2019 time bin (**Figure 4b**). During warm weekend days, the probability of exceedance has decreased from 92% in the 1972-1975 year bin to 10% in 2016-2019. On warm days, the probability of exceedance began to consistently respond to weekend decreases in NO_2* starting in the 2000-2003 time bin. By 2008-2011, it became clear that ozone chemistry on warm days was also NO_x-limited as indicated by the strong NO_2* dependence between weekends and weekdays.

On moderate days, the probability of exceedance has declined over the entire period, however there is not a clear decrease in PoE between weekdays and weekends within the same time bins. The probability of exceedance decreased by 51% on weekdays and 62% on weekends between the first time bin (1972-1975) and the final time bin (2016-2019) (**Figure 4c**). In the

most recent time bins, the probability of exceedance on moderate days approaches zero, and there is no discernable trend for the dependence of PoE on NO_2*.

The variations in the response of PoE to NO_2* indicates different sources of VOCs dominating VOCR in the three temperature regimes. For fixed concentrations of NO_2*, variations in the behavior of PoE for differing temperature bins can be used as a proxy for variations in VOCR (VOC reactivity) in the BWR (Pusede & Cohen, 2012; Nussbaumer & Cohen, 2020). When ozone chemistry is not fully NO_x-limited, ozone production is responsive to changes in VOCR. If the VOCR does not change significantly between year bins, the PoE will be relatively constant when the weekend NO_2* concentration in a later year bin is similar to the weekday NO_2* concentration in a prior time bin.

On warm and moderate days, a decrease in PoE is observed between year bins with similar values of NO_2*, signifying the dominant VOCR on warm and moderate days has decreased between 1972 and 2019 (**Figure 4b, c**). A similar decrease is not observed on hot days, indicating the dominant VOCR on hot days has not changed significantly over the same time period (**Figure 4a**). Biogenic emissions of isoprene increase with temperature and are likely the dominant component of VOCR on hot days during the entire time period (Duncan et al., 2009). Due to the strong temperature dependence of biogenic emissions, anthropogenic emissions of VOCs are relatively more important on warm and moderate temperature days. Reduced anthropogenic emissions of VOCs resulted in decreased PoE on warm and moderate days, demonstrating the important role for reductions in emission of anthropogenic VOCs, particularly for days below 31.7°C.

Reductions in anthropogenic emissions of NO_x and VOCs have driven the reduction in ozone exceedances in the BWR. On hot days, the reductions in NO_x have had the greatest effect on decreasing the number of ozone exceedances. On moderate temperature days, the reduction in PoE for data collected with similar concentrations of NO_2* concentrations in different time bins indicates that policy-driven reductions in the emission of VOCs also helped reduce ozone exceedances in the BWR. Reductions in VOCs and NO_2* both helped reduce the probability of surface ozone exceedance on warm days.

3.2 Calculating Relative Impact of Precursor Emission Reductions at an Urban Site

Ozone production as a function of NO_2 was calculated with output from a 0-D photochemical box model (Wolfe et al., 2016) constrained to the median 10 am-2 pm concentrations of VOCs and CO measured on hot days ($T \geq 31.7°C$) at an urban site in Essex, MD. The model was used to represent the same 4-year time bins as the previous section. From the model output, 10 am- 2pm average PO_3 was calculated as a function of NO_2 for each time bin (**Table 1**). The corresponding median mixing ratios of NO_2 during midday (10 am-2 pm) on hot days are represented as a closed circle for the ozone production curve of each time bin (**Figure 5**). While this model result is not an exact representation of chemistry occurring in the BWR on any given day, the analysis shown in Table 1 serves as a useful representation of the

overall trends in tropospheric ozone chemistry over the 24-year time period during which observations of VOCs are available.

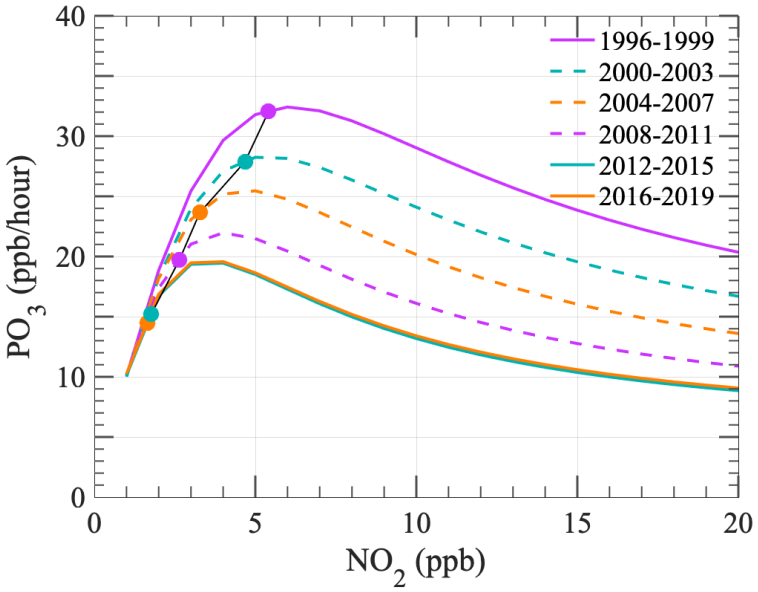

Figure 5 Model calculated ozone production rate vs. NO_2 for 1996-1999 (purple), 2000-2003 (dashed turquoise), 2004-2007 (dashed orange), 2008-2011 (dashed purple), 2012-2015 (turquoise), and 2016-2019 (orange). The corresponding median NO_2 mixing ratio estimated from observed NO_X is indicated as a closed circle for the plotted year bin.

Over the past two and a half decades (1996-2019), the typical value of daytime NO_2 on hot days has been at the peak or to the left of the peak of the corresponding ozone production curve (**Figure 5**). In the 1996-1999 time bin, the typical concentration of NO_2 was near the peak of PO_3, in a region where PO_3 does not change much with respect to the concentration of NO_2, indicating the BWR was in a transition regime during this time period. From the 2000-2003 time bin through the 2012-2015 time bin, the representative abundance of daytime NO_2 was to the left of the peak PO_3, indicating primarily NO_x -limited chemistry, with 2012-2015 being well into the NO_x-limited regime. This conclusion agrees fairly well with the analysis of the probability of

exceedance analysis, which had a transition by the 2000-2003 time-bin. The difference in time of transition may be caused by the representation of VOCs in the model being from the urban site in Essex, MD, which is expected to have higher concentrations of anthropogenic VOCs than the majority of the BWR. As NO_2 continued to decrease and ozone chemistry became even more NO_x-limited, the difference between the curves became less important because PO_3 is not affected by changing VOC concentrations at low NO_x concentrations. This effect is apparent in **Figure 5**, as the PO_3 curves do not diverge until NO_2 is greater than ~2 ppbv.

The results from our box model analysis, constrained by surface data for ozone and NO_2 acquired throughout the region and data for VOCs from the Essex site, suggest that reductions of NO_2 and VOCs have both contributed to the decrease in ozone production in the BWR. **Table 1** quantifies the calculated effect that reductions of specific species (i.e. select VOCs, CO, NO_x, and O_3) had on overall PO_3 between each consecutive time bin. For our model runs, we constrained NO_2 and O_3 to observations and allowed NO_x to vary. For a fixed concentration of NO_2, as O_3 decreases model calculated NO must increase to remain in photostationary state. Observed ozone decreased between time bins, resulting in increased PO_3 from increased NO concentrations. This result is reflected in **Table 1** where decreases in ozone are shown to increase PO_3 by a total of 1.8 ppbv/hr between the first and final complete time bins. The resulting increase of PO_3 from the runs that only perturbed constrained ozone was subtracted from the overall change in PO_3 between time bins (ΔPO_3) to calculate the percent contribution of VOC and NO_x to the reduction of PO_3 between time bins (**Table 1**).

Units: ppbv/hr	YB1-YB2	YB2-YB3	YB3-YB4	YB4-YB5	YB1-YB5
Xylenes	−1.1	−0.2	−0.4	−0.2	−0.9
HCHO	−0.2	−0.5	−0.7	−0.1	−0.8
Isoprene	−0.4	−0.4	0.0	−0.5	−0.4
Acetaldehyde	−0.5	0.0	−0.2	0.0	−0.3
CO	−0.3	0.0	−0.4	0.0	−0.2
Internal Olefins	−0.3	−0.3	0.0	0.0	−0.2
Other VOCs	−0.4	−0.1	−0.1	−0.1	−0.1
VOC Total ΔPO₃	**−3.1**	**−1.5**	**−1.8**	**−0.8**	**−2.9**
PO₃ bin 1	32.0	27.9	23.7	19.7	32.0
PO₃ bin 2	27.9	23.7	19.7	15.2	15.2
ΔPO₃	−4.1	−4.2	−4.0	−4.5	−16.8
O₃	0.1	0.5	0.4	0.4	1.8
ΔPO₃ − O₃	**−4.2**	**−4.7**	**−4.4**	**−4.9**	**−18.6**
VOC contribution	**73.8%**	**31.9%**	**40.9%**	**16.3%**	**15.6%**
NOX contribution	**26.2%**	**69.1%**	**59.1%**	**83.7%**	**84.4%**

Table 1 The calculated change in PO_3 (in ppbv/hr, rounded to the nearest tenth) for each complete 4-year time bin and the overall change between the 1996-1999 and 2012-2015 year bins (YB1-YB5) for each CB6r2 species influencing change in PO_3 for year bin change.

Focusing only on the first complete four-year long time bin (YB1, 1996-1999) and the final complete time bin (YB5, 2012-2015) minimizes the contribution of VOC reductions to lowering PO_3 (**Table 1**). However, analyzing the changes from time bin to time bin, until the most recent complete four-year long time bins (YB4, 2007-2011 and YB5, 2012-2015), reductions in VOCs contributed over 30% or more to the decrease in PO_3. Most recently, NO_x reductions are the main driver (83.7%) of PO_3 decreases, indicating the photochemical production of ozone is within the highly NO_x-limited regime in the BWR.

Over the last several decades, reductions in PO_3 in the BWR are the direct result of decreases in the abundance of ozone precursor species. **Table 1** highlights the species with the

most impact on ozone production rates. Reductions in species that are primarily anthropogenic (CO, xylenes, internal olefins, and other VOCs) contributed as much as 70% (2.1 ppbv/hr) of the ozone production decreases between the first two time bins. Although biogenic, the mixing ratio of isoprene decreased at Essex, Maryland; this decline also contributed to decreased ozone production rates. The aldehydes, primarily formaldehyde (HCHO), decreased throughout all the year bins. Since formaldehyde is both emitted and produced via VOC oxidation, this reduction may be a combined response of reduction in anthropogenic VOCs and a secondary response to having less VOCs available to oxidize (Atkinson, 1999; Parrish et al., 2012).

The large VOC contribution to the reduction of PO_3 between the YB1-YB2 suggests the BWR was sensitive to changes in VOCs during this time period, which is indicative of ozone chemistry in either the NO_x-suppressed or ozone chemistry transitioning between regimes. In the years before YB1 (before 1996), higher observed NO_2 concentrations suggest that ozone chemistry would also be sensitive to reductions in VOCs. A considerable effort to reduce VOCs in the BWR occurred prior to 1990 when anthropogenic VOCs were thought to be the dominant ozone precursor (Lebron, 1975; Wolff, 1993; Jacob, 2009). While ozone concentrations in the BWR remained well above the federal standard from 1972 to 1990, these reductions in the emission of VOCs helped facilitate the transition to the NO_x-limited regime and decrease ozone concentrations. Since the BWR began addressing the ozone problem before it was in the NO_x-limited regime, the reduction in the emission of VOCs counteracted a possible increase in urban ozone production rates that would be expected with decreasing concentrations of NO_x primarily due to federally mandated addition of catalytic converters on mobile vehicles. Furthermore, the reductions in VOCs decreased the peak rate of ozone production, which

allowed the BWR to transition to the NO_x-limited regime without experiencing a notable increase in ozone exceedance days.

The data for VOCs used in these model runs are from the PAMS monitoring site location in Essex, MD designated to measure a host of pollutants near large, local anthropogenic emissions. As a result, these model results are representative of the mainly urban areas within the BWR. The contribution of VOC reductions on PO_3 should be viewed as an upper limit for the entire region. Though, it was previously thought that VOCR in the BWR was dominated by isoprene, these results show anthropogenic VOCs and CO still have an impact on PO_3 in the BWR (McKeen et al., 1991; Li et al., 2019).While continued decreases in NO_x emissions will be most effective in obtaining compliance for the EPA ozone standard, prior emission reductions for VOC and CO have had a significant impact on improving ozone in the BWR over the past two decades..

3.3 Ozone Production Regimes in the 2011 Maryland DISCOVER-AQ campaign

Here we examine the ozone production regime based upon analysis of extensive airborne sampling over the BWR in summer 2011 during the DAQ campaign. Measurements from flight spirals during the campaign can be compared to satellite observations. The median value of $\delta PO_3/\delta NO_2$ from model output was calculated for each spiral in the boundary layer (alt.< 500 m). Of the 117 valid spirals used in this analysis, 107 (91.5%) were NO_x-limited and 10 (8.5%) spirals were classified as NO_x-saturated based upon this analysis (**Figure 6, top**). Typically, spirals classified as NO_x-saturated occurred earlier in the day, on average two hours earlier than the average time of spirals for the 2011 campaign. The NO_x-saturated spirals (and

1 their frequency) were located over Padonia (1), Fairhill (1), Edgewood (2), Essex (5), and the
2 Chesapeake Bay (1).

3 Both NO_x-saturated and NO_x-limited chemistry were observed within the boundary layer
4 for values ranging between 1.2-2.2 of tropospheric column $HCHO/NO_2$ ratios calculated from
5 DISCOVER-AQ observations. The maximum column ratio value with NO_x-saturated chemistry
6 was observed to be 2.2. Four spirals having a value for the $HCHO/NO_2$ ratio below 2.2 were
7 classified as NO_x-limited, with the lowest $HCHO/NO_2$ ratio with NO_x-limited chemistry having a
8 value of 1.2. Consequently, ratios of 1.2 to 2.2 represent a "transition" range where both types
9 of chemistry can occur, with lower values having a higher likelihood of being NO_x-saturated.

10 The data were also used to evaluate *in situ* chemistry during the 2011 DAQ campaign. Of
11 the 8139 one-minute average measurements in the boundary layer used in this analysis, 6.4%
12 were NO_x-saturated and 93.6% were NO_x-limited (**Figure 6, bottom**). Similar to the boundary
13 layer spiral observations, the average NO_x-saturated chemistry measurements occurred two
14 hours earlier than the campaign average spiral time (11 am vs 1 pm EST). The majority of the *in-*
15 *situ* 1-minute average NO_x-saturated measurements were at Essex (193), an urban site, and at
16 Beltsville (197), a site between Washington, DC and Baltimore.

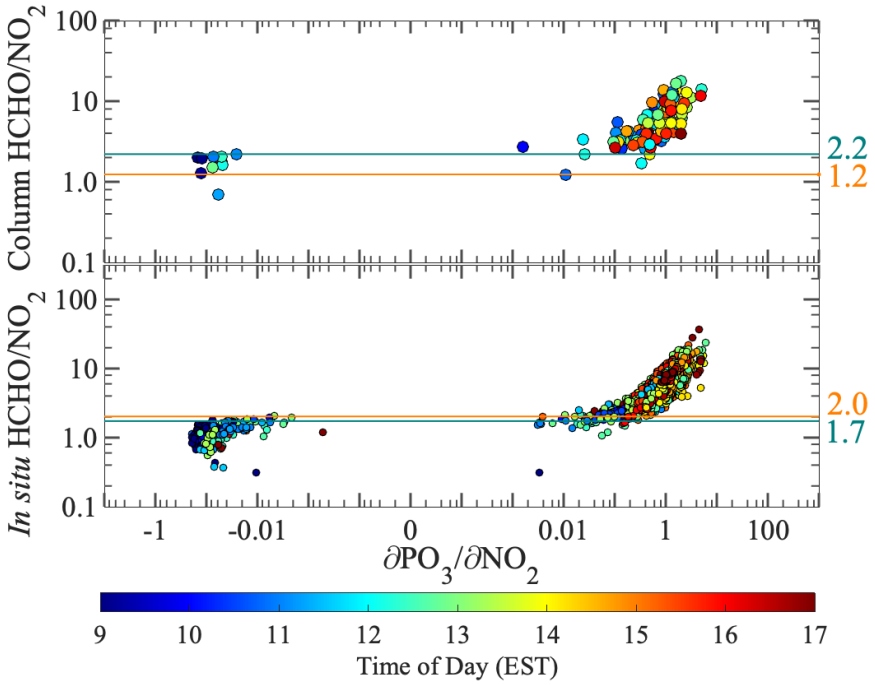

Figure 6 Model-calculated values of $\delta PO_3/\delta NO_2$ (x-axis, NO_x-saturated: negative, NO_x-limited: positive) compared with the tropospheric column $HCHO/NO_2$ ratio (top panel) and *in situ* observations of $HCHO/NO_2$ (bottom panel) in the boundary layer (alt < 500 m), both calculated from the July 2011 DAQ campaign colored by time of day. The teal line represents the top ratio value calculated within the NO_x-saturated regime (top: maximum tropospheric column ratio observation, bottom: 95% *in situ* ratio observation) and the orange line represents the bottom ratio value within the NO_x-limited regime (top: minimum tropospheric column ratio observation, bottom: 5% *in situ* ratio observation).

The DAQ campaign occurred in 2011, when Maryland was primarily NO_x-limited according to our analysis of surface data described in Section 3.1. The overlapping range of 1.2-2.2 calculated in this analysis only has a small sample size of NO_x-saturated spirals. The range of this regime may include a wider range of $HCHO/NO_2$ column ratio values if there were more NO_x-saturated spirals observed. A recent study analyzed a longer period of data (2005-2016) by correlating surface ozone concentrations at OMI overpass time with satellite tropospheric $HCHO/NO_2$ column ratio and found NO_x-suppressed chemistry may occur at ratio values up to

4.1 in the BWR (Jin et al., 2020). The aircraft sampling was also biased towards sunny days and all observations were collected in July, which does not portray a complete representation of all of the meteorological and chemical conditions during the ozone season in the BWR. However, the DAQ observations do provide insight for inferring the chemical regime from satellite observations of the June-August (JJA) $HCHO/NO_2$ column ratio in the BWR over time, which is the topic of the next section.

3.4 Satellite Observations during Surface Transition to NO_x-limited regime

Another method used to infer ozone chemistry is through satellite observations. Here, the tropospheric column $HCHO/NO_2$ ratio is assessed using the transition range calculated in section 3.3 (1.2-2.2) and compared to the ground-based observations in the BWR. Observations of HCHO and NO_2 are available from multiple satellites, with the earliest measurements starting in 1996. Since 1996, ground-based observations indicate the BWR has been increasingly sensitive to NO_x, over the same time period the June-July-August (JJA) average tropospheric column $HCHO/NO_2$ ratios have increased (**Figure 7**). The tropospheric column ratio was initially measured by GOME at 1.2 in 1996 and has since increased to an observed JJA average of 3.7 during the morning overpass from GOME-2B and 3.9 during the afternoon overpass time from OMI. The main driver behind this increase in the tropospheric column ratio is the decreasing column amounts of tropospheric NO_2. The satellite instruments used in this analysis vary in overpass time and resolution, resulting in variability in observed column ratio values in years with observations from multiple satellite instruments. The ratio values agree within the given

margin of error and all satellites show an increasing trend in ratio values, indicating the region is moving further into the NO_x-limited regime.

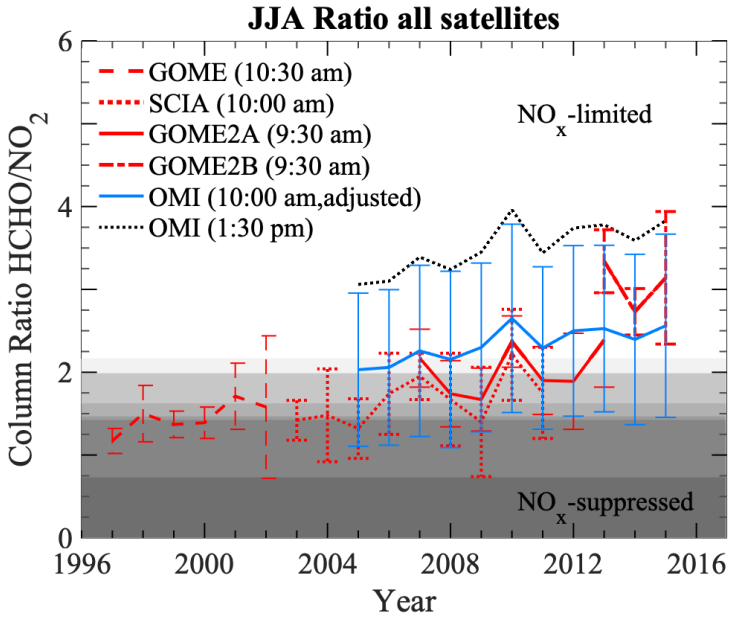

Figure 7 Average June-August (JJA) tropospheric column ratio over the Baltimore/Washington Metropolitan area for each year of available satellite data. Satellites overpass times are distinguished by color for morning (red) and afternoon adjusted to morning (blue), afternoon (dotted black). The different shades of gray represent the probability of a NO_x-saturated point at the given $HCHO/NO_2$ value using the column calculations from the July 2011 Discover-AQ flights in Maryland where the dark gray represents exclusively NO_x-saturated columns and white represents exclusively NO_x-limited columns.

The shading in **Figure 7** represents the probability of NO_x-saturated chemistry determined in the previous section using observations during the 2011 Maryland DAQ campaign, with darker shades representing a higher probability of NO_x-saturated chemistry. For the majority of the time between 1996-2016, the tropospheric column $HCHO/NO_2$ value has been between 1.2-2.2,where both NO_x-limited and NO_x-saturated chemistry occurs. These observations indicate that the predominant morning time chemistry in the BWR is in this transitional regime for this 21-year period, becoming more NO_x-limited with time. In 2010, the

morning overpass observations from satellites began to exit this transitional regime, and by 2013 all satellites were measuring a $HCHO/NO_2$ column ratio that suggests the region is predominantly NO_x-limited during during overpass times in the summer.

The observed transition to the NO_x-limited regime inferred from satellite observations (2010) was much later than the time frame of transition suggested by the ground-based observations (**Figure 7**). However, the satellite overpass time is typically in the morning (between 9:30 and 10:30 am), during a time when HO_x concentrations are low due to the solar zenith angle dependence of the production of $O(^1D)$ from the photolysis of ozone. Higher HO_x concentrations in the afternoon combined with increased biogenic VOC emissions result in higher ozone production in the early afternoon. Morning satellite observations are not ideal for deducing the ozone production regime during the peak of ozone production. The diurnal variation of HCHO andNO_2 would likely result in higher values of $HCHO/NO_2$ ratios, or more NO_x-limited chemistry, in the afternoon (Jin et al., 2020; Souri et al., 2020).

Afternoon observations of tropospheric column $HCHO/NO_2$ from the OMI instrument are consistently higher than the observations from satellites with morning overpass times (**Figure 7**). The entire time series of available observations from OMI exhibit values of the $HCHO/NO_2$ ratio that are above 2.1, indicating the BWR has been primarily NO_x-limited at 1:30 pm, the approximate time of the afternoon overpass, since at least 2005. The analysis of DAQ observations in Section 3.3 showed a similar increase in the column $HCHO/NO_2$ ratio between morning and afternoon. These results demonstrate that satellite observations of column $HCHO/NO_2$ can reflect annual trends and diurnal variations in ozone chemistry. Newly launched

and planned geostationary satellites (TEMPO, Sentinel-4, and GEMS) will provide higher temporal and spatial resolution for the observations of HCHO and NO_2 and allow for further investigation of the use of satellite observations to infer changes in surface ozone chemistry.

4. Summary

Ground-based and satellite observations over the Baltimore-Washington Metropolitan region (BWR) indicate the dominant chemical regime for ozone production in the BWR has been NO_x-limited on hot days since the 2000-2003 time bin. This transition period is inferred from three analysis methods: the response of reduced NO_x on weekends on probability of exceedance (PoE), a data-constrained box model, and the satellite time series of tropospheric column ratio of HCHO/NO_2. Beginning in the 2000-2003 time bin, weekend PoE probability was consistently lower than weekday PoE, signifying ozone chemistry was NO_x-limited. The box model output indicates that since the 1996-1999 time bin median NO_2 mixing ratios were to the left of the peak of the corresponding time bin's ozone production curve, representing NO_x-limited chemistry. The NO_x-limited chemistry resulted in large reductions in ozone exceedance probability as a response to NO_x reductions that have occurred since 2004. Output from box model runs was analyzed for the impact of VOC, CO, and NO_2 reductions on ozone production rates at a site near Baltimore between 1996-2019. Model output demonstrates the region is currently highly sensitive to changes in NO_x concentrations, but reductions in VOCs contributed to over 30% of the decrease in PO_3 until 2008. Observations of tropospheric column ratio HCHO/NO_2 in grid cells over the BWR are currently above 2.1 for all operating satellites since 2010, signifying the region is primarily NO_x-limited even in the morning. Afternoon satellite

observations of tropospheric column $HCHO/NO_2$ from OMI are currently well into the NO_x-limited regime and have been NO_x-limited for the entire OMI time series (2005-2016). All parts of this analysis indicate that the BWR has been dominated by NOx-limited chemistry since the early 2000s and that continued decreases in the emission of NOx will slow the rate of ozone production to help the region move towards compliance with the surface ozone standard.

While NO_x reductions were the driving factor behind the dramatic improvement in ozone air quality in the BWR over the last two decades, VOC reductions also had a noticeable impact in improving air quality the BWR, especially at urban sites. The majority of VOC reductions were before 1996 (Fiore et al., 1998; Hidy & Blanchard, 2015), so those reductions likely had larger contributions to controlling ozone production, especially in urban areas (Lebron, 1975; Korsog & Wolff, 1991; Wolff, 1993). Reductions in VOCs and CO also helped lower the peak height of ozone production, saving the BWR from worse air quality as the region transitioned to NO_x-limited chemistry. The differences in PoE between weekdays and weekends on moderate temperature days ($26.1°C \leq T < 28.9°C$) and warm days ($28.9°C \leq T < 31.7°C$) suggest that the reduction of VOCs and CO have helped decrease the number of exceedances on warm days and nearly eliminated exceedances in the region on moderate days.

This multi-faceted analysis was used to evaluate a region formerly plagued with severe air quality issues that has been successful in implementing policies to decrease the number of ozone exceedances (He et al., 2013b; Aburn et al., 2015). The response of ozone exceedances to air quality policies can help give insight into a region with evolving chemistry through a transition from NO_x-saturated to NO_x-limited chemistry. This analysis indicates that VOC reductions in urban regions that have yet to transition or are in the process of transitioning are

important to prevent increasing surface ozone during the transition. Furthermore, current day-of-week variations in the BWR indicate that ozone production in the region is highly dependent on the abundance of NO_x. While early reductions to ozone precursors pushed the BWR close to the chemical transition point, the regional reductions in NO_x from emission controls on EGUs lowered NO_x concentrations enough for the chemistry to become primarily NO_x-limited in the BWR.

While the BWR has had significant improvements in air quality over the past two decades, the region still has not met the EPA standard for ozone. The strongly NO_x-limited chemistry in the BWR suggests that further reductions in NO_x will lead to a significant decrease in ozone. Continued decreases in ozone allows for improvements in public health and ease reaching attainment for any future changes to the EPA standard for ozone. One possible target is diesel truck emissions, which appear to influence strongly the day-of-week variations in observed NO_2*. If emissions from these vehicles are decreased to the current weekend levels, the weekday exceedance probability could fall by 30% in a given year. The methods used in this research make use of data collected in many nonattainment regions of the U.S. This analysis may be applied to provide further insight into changing ozone chemistry in nonattainment regions, allowing for more scientifically-informed policies to bring these areas into compliance with the EPA's ozone standard.

5. Acknowledgments

We thank the Maryland Department of the Environment (MDE) for support of the Regional Atmospheric Measurement Modeling and Prediction Program (RAMMPP; Grant #

U00P8400705), the National Aeronautics and Space Administration for support of the Atmospheric Composition and Modeling Program (ACMAP, Grant # 80NSSC19K0983), and the National Aeronautics and Space Administration for support of Atmospheric Composition Campaign Data Analysis and Modeling (ACCDAM, Grant # 20-ACCDAM20-0044). We acknowledge free use of data used in this research from the EPA AQS, EPA AMPD, NASA DISCOVER-AQ, and NOAA CDO programs. We also acknowledge the free use of tropospheric NO_2 column data and HCHO column data from the GOME, SCIAMACHY, GOME-2, and OMI sensors from www.temis.nl. We thank Barry Balzanna and the Maryland State Highway Administration for providing traffic data along I-95 in MD and Yu Gao and the Department of Transportation Planning of the Metropolitan Washington Council of Governments for traffic data along DC-295. Finally, we thank Xinrong Ren for assistance in the initial phase of this project and Dan Goldberg for providing CAMx model output for analysis.

6. References

Aburn, G., Dickerson, R. R., & Canty, T. P. (2015). A Path Forward for the Eastern United States. *Environmental Manager*, (May), 18–24.

Anderson, D. C., Loughner, C. P., Diskin, G. S., Weinheimer, A. J., Canty, T. P., Salawitch, R. J., et al. (2014). Measured and modeled CO and NO y in DISCOVER-AQ: An evaluation of emissions and chemistry over the eastern US. *Atmospheric Environment*, *96*, 78–87. https://doi.org/10.1016/j.atmosenv.2014.07.004

Atkinson, R. (1999). Reactive Hydrocarbons in the Atmosphere. *Eos, Transactions American Geophysical Union*, *80*(15), 176. https://doi.org/10.1029/99EO00127

Ban-Weiss, G. A., McLaughlin, J. P., Harley, R. A., Lunden, M. M., Kirchstetter, T. W., Kean, A. J., et al. (2008). Long-term changes in emissions of nitrogen oxides and particulate matter from on-road gasoline and diesel vehicles. *Atmospheric Environment*, *42*(2), 220–232. https://doi.org/10.1016/j.atmosenv.2007.09.049

Bednarz, F. (1995). The GOME Users Manual.

Bell, M. L., Peng, R. D., & Dominici, F. (2006). The Exposure–Response Curve for Ozone and Risk of Mortality and the Adequacy of Current Ozone Regulations. *Environmental Health Perspectives*, *114*(4), 532–536. https://doi.org/10.1289/ehp.8816

Blanchard, C. L., Tanenbaum, S., & Lawson, D. R. (2008). Differences between Weekday and Weekend Air Pollutant Levels in Atlanta; Baltimore; Chicago; Dallas–Fort Worth; Denver; Houston; New York; Phoenix; Washington, DC; and Surrounding Areas. *Journal of the Air & Waste Management Association*, *58*(12), 1598–1615. https://doi.org/10.3155/1047-3289.58.12.1598

Bloomer, B. J., Stehr, J. W., Piety, C. A., Salawitch, R. J., & Dickerson, R. R. (2009). Observed relationships of ozone air pollution with temperature and emissions. *Geophysical Research Letters*, *36*(9), L09803. https://doi.org/10.1029/2009GL037308

Boersma, K. F., Eskes, H. J., & Brinksma, E. J. (2004). Error analysis for tropospheric NO 2 retrieval from space. *Journal of Geophysical Research: Atmospheres*, *109*(D4), n/a-n/a. https://doi.org/10.1029/2003JD003962

Boersma, K. F., Eskes, H. J., Dirksen, R. J., van der A, R. J., Veefkind, J. P., Stammes, P., et al. (2011). An improved tropospheric NO₂ column retrieval algorithm for the Ozone Monitoring Instrument. *Atmospheric Measurement Techniques*, *4*(9), 1905–1928. https://doi.org/10.5194/amt-4-1905-2011

Bovensmann, H., Burrows, J. P., Buchwitz, M., Frerick, J., Noël, S., Rozanov, V. V., et al. (1999). SCIAMACHY: Mission Objectives and Measurement Modes. *Journal of the Atmospheric Sciences*, *56*(2), 127–150. https://doi.org/10.1175/1520-0469(1999)056<0127:SMOAMM>2.0.CO;2

Brent, L. C., Thorn, W. J., Gupta, M., Leen, B., Stehr, J. W., He, H., et al. (2015). Evaluation of the use of a commercially available cavity ringdown absorption spectrometer for measuring NO2 in flight, and observations over the Mid-Atlantic States, during DISCOVER-AQ. *Journal of Atmospheric Chemistry*, *72*(3–4), 503–521. https://doi.org/10.1007/s10874-013-9265-6

Burrows, J. P., Weber, M., Buchwitz, M., Rozanov, V. V., Ladstätter-Weißenmayer, A., Richter, A., et al. (1999). The Global Ozone Monitoring Experiment (GOME): Mission Concept and First Scientific Results. *Journal of the Atmospheric Sciences*, *56*(2), 151–175. https://doi.org/10.1175/1520-0469(1999)056<0151:TGOMEG>2.0.CO;2

Callies, J., Corpaccioli, E., Eisinger, M., Hahne, A., & Lefebvre, A. (2000). GOME-2-Metop's second-generation sensor for operational ozone monitoring. *ESA Bulletin*, *102*(may), 28–36.

Canty, T. P., Hembeck, L., Vinciguerra, T. P., Anderson, D. C., Goldberg, D. L., Carpenter, S. F., et al. (2015). Ozone and NO_{<i>x</i>} chemistry in the eastern US: evaluation of CMAQ/CB05 with satellite (OMI) data. *Atmospheric Chemistry and Physics*, *15*(19), 10965–10982. https://doi.org/10.5194/acp-15-10965-2015

Chameides, W. L., & Walker, J. C. G. (1973). A photochemical theory of tropospheric ozone. *Journal of Geophysical Research*, *78*(36), 8751–8760. https://doi.org/10.1029/JC078i036p08751

Chameides, W. L., Lindsay, R. W., Richardson, J., & Kiang, C. S. (1988). The Role of Biogenic Hydrocarbons in Urban Photochemical Smog: Atlanta as a Case Study. *Science*, *241*(4872), 1473–1475. https://doi.org/10.1126/science.3420404

Crutzen, P. J. (1971). Ozone production rates in an oxygen-hydrogen-nitrogen oxide

atmosphere. *Journal of Geophysical Research*, *76*(30), 7311–7327. https://doi.org/10.1029/JC076i030p07311

Crutzen, P. J. (1973). A discussion of the chemistry of some minor constituents in the stratosphere and troposphere. *Pure and Applied Geophysics*, *106–108*(1), 1385–1399. https://doi.org/10.1007/BF00881092

Dallmann, T. R., & Harley, R. A. (2010). Evaluation of mobile source emission trends in the United States. *Journal of Geophysical Research*, *115*(D14), D14305. https://doi.org/10.1029/2010JD013862

Devlin, R. B., Duncan, K. E., Jardim, M., Schmitt, M. T., Rappold, A. G., & Diaz-Sanchez, D. (2012). Controlled Exposure of Healthy Young Volunteers to Ozone Causes Cardiovascular Effects. *Circulation*, *126*(1), 104–111. https://doi.org/10.1161/CIRCULATIONAHA.112.094359

Dickerson, R. R., Anderson, D. C., & Ren, X. (2019). On the use of data from commercial NOx analyzers for air pollution studies. *Atmospheric Environment*, *214*(June), 116873. https://doi.org/10.1016/j.atmosenv.2019.116873

Duncan, B. N., Yoshida, Y., Damon, M. R., Douglass, A. R., & Witte, J. C. (2009). Temperature dependence of factors controlling isoprene emissions. *Geophysical Research Letters*, *36*(5), L05813. https://doi.org/10.1029/2008GL037090

Duncan, B. N., Yoshida, Y., Olson, J. R., Sillman, S., Martin, R. V., Lamsal, L. N., et al. (2010). Application of OMI observations to a space-based indicator of NOx and VOC controls on surface ozone formation. *Atmospheric Environment*, *44*(18), 2213–2223. https://doi.org/10.1016/j.atmosenv.2010.03.010

Dunlea, E. J., Herndon, S. C., Nelson, D. D., Volkamer, R. M., San Martini, F., Sheehy, P. M., et al. (2007). Evaluation of nitrogen dioxide chemiluminescence monitors in a polluted urban environment. *Atmospheric Chemistry and Physics*, *7*(10), 2691–2704. https://doi.org/10.5194/acp-7-2691-2007

EPA. (1996). *National Air Quality and Emissions Trends Report, 1996*.

EPA. (2014). Health risk and exposure assessment for ozone, 1–502. https://doi.org/EPA-452/R-14-004a

EPA Green Book, E. (2019). No Title. *EPA Green Book, 8-Hour Ozone (2015) Designated Area/State Information*.

Fehsenfeld, F. C., Drummond, J. W., Roychowdhury, U. K., Galvin, P. J., Williams, E. J., Buhr, M. P., et al. (1990). Intercomparison of NO 2 measurement techniques. *Journal of Geophysical Research*, *95*(D4), 3579. https://doi.org/10.1029/JD095iD04p03579

Fiore, A. M., Jacob, D. J., Logan, J. A., & Yin, J. H. (1998). Long-term trends in ground level ozone over the contiguous United States, 1980-1995. *Journal of Geophysical Research: Atmospheres*, *103*(D1), 1471–1480. https://doi.org/10.1029/97JD03036

Flynn, C. M., Pickering, K. E., Crawford, J. H., Lamsal, L. N., Krotkov, N. A., Herman, J. R., et al. (2014). Relationship between column-density and surface mixing ratio: Statistical analysis of O3 and NO2 data from the July 2011 Maryland DISCOVER-AQ mission. *Atmospheric Environment*, *92*, 429–441. https://doi.org/10.1016/j.atmosenv.2014.04.041

Frost, G. J., McKeen, S. A., Trainer, M., Ryerson, T. B., Neuman, J. A., Roberts, J. M., et al. (2006). Effects of changing power plant NO x emissions on ozone in the eastern United States: Proof of concept. *Journal of Geophysical Research*, *111*(D12), D12306.

https://doi.org/10.1029/2005JD006354
Gao, H. O. (2007). Day of week effects on diurnal ozone/NOx cycles and transportation emissions in Southern California. *Transportation Research Part D: Transport and Environment*, *12*(4), 292–305. https://doi.org/10.1016/j.trd.2007.03.004
Gilliland, A. B., Hogrefe, C., Pinder, R. W., Godowitch, J. M., Foley, K. L., & Rao, S. T. (2008). Dynamic evaluation of regional air quality models: Assessing changes in O3 stemming from changes in emissions and meteorology. *Atmospheric Environment*, *42*(20), 5110–5123. https://doi.org/10.1016/j.atmosenv.2008.02.018
Godowitch, J. M., Gilliland, A. B., Draxler, R. R., & Rao, S. T. (2008). Modeling assessment of point source NOx emission reductions on ozone air quality in the eastern United States. *Atmospheric Environment*, *42*(1), 87–100. https://doi.org/10.1016/j.atmosenv.2007.09.032
Goldberg, D. L., Vinciguerra, T. P., Hosley, K. M., Loughner, C. P., Canty, T. P., Salawitch, R. J., & Dickerson, R. R. (2015). Evidence for an increase in the ozone photochemical lifetime in the eastern United States using a regional air quality model. *Journal of Geophysical Research: Atmospheres*, *120*(24), 12778–12793. https://doi.org/10.1002/2015JD023930
Goldberg, D. L., Vinciguerra, T. P., Anderson, D. C., Hembeck, L., Canty, T. P., Ehrman, S. H., et al. (2016). CAMx ozone source attribution in the eastern United States using guidance from observations during DISCOVER-AQ Maryland. *Geophysical Research Letters*, *43*(5), 2249–2258. https://doi.org/10.1002/2015GL067332
Grosjean, D., & Harrison, J. (1985). Response of chemiluminescence NOx analyzers and ultraviolet ozone analyzers to organic air pollutants. *Environmental Science & Technology*, *19*(9), 862–865. https://doi.org/10.1021/es00139a016
Gryparis, A., Forsberg, B., Katsouyanni, K., Analitis, A., Touloumi, G., Schwartz, J., et al. (2004). Acute Effects of Ozone on Mortality from the "Air Pollution and Health. *American Journal of Respiratory and Critical Care Medicine*, *170*(10), 1080–1087. https://doi.org/10.1164/rccm.200403-333OC
Hains, J. C., Taubman, B. F., Thompson, A. M., Stehr, J. W., Marufu, L. T., Doddridge, B. G., & Dickerson, R. R. (2008). Origins of chemical pollution derived from Mid-Atlantic aircraft profiles using a clustering technique. *Atmospheric Environment*, *42*(8), 1727–1741. https://doi.org/10.1016/j.atmosenv.2007.11.052
Hall, D. L., Anderson, D. C., Martin, C. R., Ren, X., Salawitch, R. J., He, H., et al. (2020). Using near-road observations of CO, NOy, and CO2 to investigate emissions from vehicles: Evidence for an impact of ambient temperature and specific humidity. *Atmospheric Environment*, *232*, 117558. https://doi.org/10.1016/j.atmosenv.2020.117558
He, H., Hembeck, L., Hosley, K. M., Canty, T. P., Salawitch, R. J., & Dickerson, R. R. (2013a). High ozone concentrations on hot days: The role of electric power demand and NO x emissions. *Geophysical Research Letters*, *40*(19), 5291–5294. https://doi.org/10.1002/grl.50967
He, H., Stehr, J. W., Hains, J. C., Krask, D. J., Doddridge, B. G., Vinnikov, K. Y., et al. (2013b). Trends in emissions and concentrations of air pollutants in the lower troposphere in the Baltimore/Washington airshed from 1997 to 2011. *Atmospheric Chemistry and Physics*, *13*(15), 7859–7874. https://doi.org/10.5194/acp-13-7859-2013
Hembeck, L., He, H., Vinciguerra, T. P., Canty, T. P., Dickerson, R. R., Salawitch, R. J., & Loughner, C. P. (2019). Measured and modelled ozone photochemical production in the Baltimore-

Washington airshed. *Atmospheric Environment: X*, *2*(February), 100017. https://doi.org/10.1016/j.aeaoa.2019.100017

Heuss, J. M., Kahlbaum, D. F., & Wolff, G. T. (2003). Weekday/Weekend Ozone Differences: What Can We Learn from Them? *Journal of the Air & Waste Management Association*, *53*(7), 772–788. https://doi.org/10.1080/10473289.2003.10466227

Hidy, G. M., & Blanchard, C. L. (2015). Precursor reductions and ground-level ozone in the Continental United States. *Journal of the Air and Waste Management Association*, *65*(10), 1261–1282. https://doi.org/10.1080/10962247.2015.1079564

Hildebrandt-Ruiz, L., & Yarwood, G. (2013). *Interactions between organic aerosol and NOy: Influence on oxidant production. Final report for AQRP project 12–012. Prepared for the Texas Air Quality Research Program.*

Horowitz, L. W., Fiore, A. M., Milly, G. P., Cohen, R. C., Perring, A., Wooldridge, P. J., et al. (2007). Observational constraints on the chemistry of isoprene nitrates over the eastern United States. *Journal of Geophysical Research*, *112*(D12), D12S08. https://doi.org/10.1029/2006JD007747

Jacob, D. J. (2009). CHAPTER 2: Aerosols. *Acta Medica Scandinavica*, *133*(S228), 6–10. https://doi.org/10.1111/j.0954-6820.1949.tb11329.x

Jacob, D. J., Logan, J. A., Gardner, G. M., Yevich, R. M., Spivakovsky, C. M., Wofsy, S. C., et al. (1993). Factors regulating ozone over the United States and its export to the global atmosphere. *Journal of Geophysical Research*, *98*(D8), 14817. https://doi.org/10.1029/98JD01224

Jacob, D. J., Horowitz, L. W., Munger, J. W., Heikes, B. G., Dickerson, R. R., Artz, R. S., & Keene, W. C. (1995). Seasonal transition from NOx- to hydrocarbon-limited conditions for ozone production over the eastern United States in September. *Journal of Geophysical Research: Atmospheres*, *100*(D5), 9315–9324. https://doi.org/10.1029/94JD03125

Jaffe, D. A., Cooper, O. R., Fiore, A. M., Henderson, B. H., Tonnesen, G. S., Russell, A. G., et al. (2018). Scientific assessment of background ozone over the U.S.: Implications for air quality management. *Elementa: Science of the Anthropocene*, *6*(56), 1–30. https://doi.org/10.1525/elementa.309

Jin, X., Fiore, A. M., Boersma, K. F., Smedt, I. De, & Valin, L. C. (2020). Inferring Changes in Summertime Surface Ozone–NO x –VOC Chemistry over U.S. Urban Areas from Two Decades of Satellite and Ground-Based Observations. *Environmental Science & Technology*, *54*(11), 6518–6529. https://doi.org/10.1021/acs.est.9b07785

Kaynak, B., Hu, Y., Martin, R. V., Sioris, C. E., & Russell, A. G. (2009). Comparison of weekly cycle of NO 2 satellite retrievals and NO x emission inventories for the continental United States. *Journal of Geophysical Research*, *114*(D5), D05302. https://doi.org/10.1029/2008JD010714

Kleinman, L. I. (2005). The dependence of tropospheric ozone production rate on ozone precursors. *Atmospheric Environment*, *39*(3), 575–586. https://doi.org/10.1016/j.atmosenv.2004.08.047

Kleinman, L. I., Daum, P. H., Lee, J. H., Lee, Y.-N., Nunnermacker, L. J., Springston, S. R., et al. (1997). Dependence of ozone production on NO and hydrocarbons in the troposphere. *Geophysical Research Letters*, *24*(18), 2299–2302. https://doi.org/10.1029/97GL02279

Korsog, P. E., & Wolff, G. T. (1991). An examination of urban ozone trends in the Northeastern

U.S. (1973-1983) using a robust statistical method. *Atmospheric Environment. Part B, Urban Atmosphere*, *25*(1), 47–57. https://doi.org/10.1016/0957-1272(91)90039-H

Lebron, F. (1975). A comparison of weekend-weekday ozone and hydrocarbon concentrations in the Baltimore-Washington metropolitan area. *Atmospheric Environment (1967)*, *9*(9), 861–863. https://doi.org/10.1016/0004-6981(75)90046-3

Levelt, P. F., Hilsenrath, E., Leppelmeier, G. W., Oord, G. H. J. Van Den, Bhartia, P. K., Tamminen, J., et al. (2006a). Monitoring Instrument, *44*(5), 1199–1208.

Levelt, P. F., van den Oord, G. H. J., Dobber, M. R., Malkki, A., Huib Visser, Johan de Vries, et al. (2006b). The ozone monitoring instrument. *IEEE Transactions on Geoscience and Remote Sensing*, *44*(5), 1093–1101. https://doi.org/10.1109/TGRS.2006.872333

Levy, H. (1972). Photochemistry of the lower troposphere. *Planetary and Space Science*, *20*(6), 919–935. https://doi.org/10.1016/0032-0633(72)90177-8

Li, J., Wang, Y., & Qu, H. (2019). Dependence of Summertime Surface Ozone on NO x and VOC Emissions Over the United States: Peak Time and Value. *Geophysical Research Letters*, *46*(6), 3540–3550. https://doi.org/10.1029/2018GL081823

Lin, X., Trainer, M., & Liu, S. C. (1988). On the nonlinearity of the tropospheric ozone production. *Journal of Geophysical Research*, *93*(D12), 15879. https://doi.org/10.1029/JD093iD12p15879

Mao, J., Ren, X., Chen, S., Brune, W. H., Chen, Z., Martinez, M., et al. (2010). Atmospheric oxidation capacity in the summer of Houston 2006: Comparison with summer measurements in other metropolitan studies. *Atmospheric Environment*, *44*(33), 4107–4115. https://doi.org/10.1016/j.atmosenv.2009.01.013

Marr, L. C., & Harley, R. A. (2002). Modeling the Effect of Weekday−Weekend Differences in Motor Vehicle Emissions on Photochemical Air Pollution in Central California. *Environmental Science & Technology*, *36*(19), 4099–4106. https://doi.org/10.1021/es020629x

Martin, R. V., Fiore, A. M., & Van Donkelaar, A. (2004). Space-based diagnosis of surface ozone sensitivity to anthropogenic emissions. *Geophysical Research Letters*, *31*(6), n/a-n/a. https://doi.org/10.1029/2004GL019416

McConnell, V. D., & Schwab, R. M. (1990). The Impact of Environmental Regulation on Industry Location Decisions: The Motor Vehicle Industry. *Land Economics*, *66*(1), 67. https://doi.org/10.2307/3146684

McDonald, B. C., Dallmann, T. R., Martin, E. W., & Harley, R. A. (2012). Long-term trends in nitrogen oxide emissions from motor vehicles at national, state, and air basin scales. *Journal of Geophysical Research: Atmospheres*, *117*(D21), n/a-n/a. https://doi.org/10.1029/2012JD018304

McDonald, B. C., Gentner, D. R., Goldstein, A. H., & Harley, R. A. (2013). Long-Term Trends in Motor Vehicle Emissions in U.S. Urban Areas. *Environmental Science & Technology*, *47*(17), 10022–10031. https://doi.org/10.1021/es401034z

McKeen, S. A., Hsie, E.-Y., & Liu, S. C. (1991). A study of the dependence of rural ozone on ozone precursors in the eastern United States. *Journal of Geophysical Research*, *96*(D8), 15377. https://doi.org/10.1029/91JD01282

Milford, J. B., Gao, D., Sillman, S., Blossey, P., & Russell, A. G. (1994). Total reactive nitrogen (NO

y) as an indicator of the sensitivity of ozone to reductions in hydrocarbon and NO x emissions. *Journal of Geophysical Research*, *99*(D2), 3533. https://doi.org/10.1029/93JD03224

Monks, P. S. (2005). Gas-phase radical chemistry in the troposphere. *Chemical Society Reviews*, *34*(5), 376. https://doi.org/10.1039/b307982c

Mudway, I. (2000). Ozone and the lung: a sensitive issue. *Molecular Aspects of Medicine*, *21*(1–2), 1–48. https://doi.org/10.1016/S0098-2997(00)00003-0

Munro, R., Lang, R., Klaes, D., Poli, G., Retscher, C., Lindstrot, R., et al. (2016). The GOME-2 instrument on the Metop series of satellites: instrument design, calibration, and level 1 data processing – an overview. *Atmospheric Measurement Techniques*, *9*(3), 1279–1301. https://doi.org/10.5194/amt-9-1279-2016

Murphy, J. G., Day, D. A., Cleary, P. A., Wooldridge, P. J., Millet, D. B., Goldstein, A. H., & Cohen, R. C. (2007). The weekend effect within and downwind of Sacramento – Part 1: Observations of ozone, nitrogen oxides, and VOC reactivity. *Atmospheric Chemistry and Physics*, *7*(20), 5327–5339. https://doi.org/10.5194/acp-7-5327-2007

NASA/LARC/SD/ASDC. (2014). DISCOVER-AQ P-3B Aircraft in-situ Trace Gas Measurements. NASA Langley Atmospheric Science Data Center DAAC. Retrieved from https://doi.org/10.5067/AIRCRAFT/DISCOVER-AQ/AEROSOL-TRACEGAS

Nussbaumer, C. M., & Cohen, R. C. (2020). The Role of Temperature and NO x in Ozone Trends in the Los Angeles Basin. *Environmental Science & Technology*, *54*(24), 15652–15659. https://doi.org/10.1021/acs.est.0c04910

Nussbaumer, C. M., & Cohen, R. C. (2021). Impact of OA on the temperature dependence of PM 2.5 in the Los Angeles basin. *Environmental Science and Technology*, *55*(6), 3549–3558. https://doi.org/10.1021/ACS.EST.0C07144

Parrish, D. D., & Ennis, C. A. (2019). Estimating background contributions and US anthropogenic enhancements to maximum ozone concentrations in the northern US. *Atmospheric Chemistry and Physics*, *19*(19), 12587–12605. https://doi.org/10.5194/acp-19-12587-2019

Parrish, D. D., Ryerson, T. B., Mellqvist, J., Johansson, J., Fried, A., Richter, D., et al. (2012). Primary and secondary sources of formaldehyde in urban atmospheres: Houston Texas region. *Atmospheric Chemistry and Physics*, *12*(7), 3273–3288. https://doi.org/10.5194/acp-12-3273-2012

Pegues, A. H., Cohan, D. S., Digar, A., Douglass, C., & Wilson, R. S. (2012). Efficacy of recent state implementation plans for 8-hour ozone. *Journal of the Air & Waste Management Association*, *62*(2), 252–261. https://doi.org/10.1080/10473289.2011.646049

Pratapas, J. M., & Calcagni, J. (1983). Ozone control strategies in the United States. *Environment International*, *9*(6), 529–538. https://doi.org/10.1016/0160-4120(83)90009-0

Pun, B. K., Seigneur, C., & White, W. (2003). Day-of-Week Behavior of Atmospheric Ozone in Three U.S. Cities. *Journal of the Air & Waste Management Association*, *53*(7), 789–801. https://doi.org/10.1080/10473289.2003.10466231

Pusede, S. E., & Cohen, R. C. (2012). On the observed response of ozone to NO_x and VOC reactivity reductions in San Joaquin Valley California 1995–present. *Atmospheric Chemistry and Physics*, *12*(18), 8323–8339. https://doi.org/10.5194/acp-12-8323-2012

Pusede, S. E., Steiner, A. L., & Cohen, R. C. (2015). Temperature and Recent Trends in the Chemistry of Continental Surface Ozone. *Chemical Reviews*, *115*(10), 3898–3918. https://doi.org/10.1021/cr5006815

Ren, X., Van Duin, D., Cazorla, M., Chen, S., Mao, J., Zhang, L., et al. (2013). Atmospheric oxidation chemistry and ozone production: Results from SHARP 2009 in Houston, Texas. *Journal of Geophysical Research Atmospheres*, *118*(11), 5770–5780. https://doi.org/10.1002/jgrd.50342

Ring, A. M., Canty, T. P., Anderson, D. C., Vinciguerra, T. P., He, H., Goldberg, D. L., et al. (2018). Evaluating commercial marine emissions and their role in air quality policy using observations and the CMAQ model. *Atmospheric Environment*, *173*(October 2017), 96–107. https://doi.org/10.1016/j.atmosenv.2017.10.037

Ruiz, L. H., & Yarwood, G. (2013). *Interactions between Organic Aerosol and NOy : Influence on Oxidant Production. Prepared for the Texas AQRP (Project 12-012).* Retrieved from http://aqrp.ceer.utexas.edu/projectinfoFY12_13/12-012/12-012 Final Report.pdf

Ryan, W. F., Doddridge, B. G., Dickerson, R. R., Morales, R. M., Hallock, K. A., Roberts, P. T., et al. (1998). Pollutant Transport During a Regional O 3 Episode in the Mid-Atlantic States. *Journal of the Air & Waste Management Association*, *48*(9), 786–797. https://doi.org/10.1080/10473289.1998.10463737

Schroeder, J. R., Crawford, J. H., Fried, A., Walega, J. G., Weinheimer, A. J., Wisthaler, A., et al. (2017). New insights into the column CH 2 O/NO 2 ratio as an indicator of near-surface ozone sensitivity. *Journal of Geophysical Research: Atmospheres*, *122*(16), 8885–8907. https://doi.org/10.1002/2017JD026781

Shen, L., & Mickley, L. J. (2017). Effects of El Niño on Summertime Ozone Air Quality in the Eastern United States. *Geophysical Research Letters*, *44*(24), 12,543-12,550. https://doi.org/10.1002/2017GL076150

Shen, L., Mickley, L. J., Leibensperger, E. M., & Li, M. (2017). Strong Dependence of U.S. Summertime Air Quality on the Decadal Variability of Atlantic Sea Surface Temperatures. *Geophysical Research Letters*, *44*(24), 12,527-12,535. https://doi.org/10.1002/2017GL075905

Sillman, S. (1995). The use of NOy, H2O2, and HNO3 as indicators for ozone-NOx-hydrocarbon sensitivity in urband locations. *Journal of Geophysical Research*, *100*(D7), 175–188.

Sillman, S., Logan, J. A., & Wofsy, S. C. (1990). The sensitivity of ozone to nitrogen oxides and hydrocarbons in regional ozone episodes. *Journal of Geophysical Research*, *95*(D2), 1837. https://doi.org/10.1029/JD095iD02p01837

Simon, H., Reff, A., Wells, B., Xing, J., & Frank, N. (2015). Ozone Trends Across the United States over a Period of Decreasing NOx and VOC Emissions. *Environmental Science & Technology*, *49*(1), 186–195. https://doi.org/10.1021/es504514z

Souri, A. H., Nowlan, C. R., Wolfe, G. M., Lamsal, L. N., Chan Miller, C. E., Abad, G. G., et al. (2020). Revisiting the effectiveness of HCHO/NO2 ratios for inferring ozone sensitivity to its precursors using high resolution airborne remote sensing observations in a high ozone episode during the KORUS-AQ campaign. *Atmospheric Environment*, *224*, 117341. https://doi.org/10.1016/j.atmosenv.2020.117341

Trainer, M., Williams, E. J., Parrish, D. D., Buhr, M. P., Allwine, E. J., Westberg, H. H., et al.

(1987). Models and observations of the impact of natural hydrocarbons on rural ozone. *Nature*, *329*(6141), 705–707. https://doi.org/10.1038/329705a0

Travis, K. R., Jacob, D. J., Fisher, J. A., Kim, P. S., Marais, E. A., Zhu, L., et al. (2016). Why do models overestimate surface ozone in the Southeast United States? *Atmospheric Chemistry and Physics*, *16*(21), 13561–13577. https://doi.org/10.5194/acp-16-13561-2016

W. Kirchstetter, T., Harley, R. A., Kreisberg, N. M., Stolzenburg, M. R., & Hering, S. V. (1999). On-road measurement of fine particle and nitrogen oxide emissions from light- and heavy-duty motor vehicles. *Atmospheric Environment*, *33*(18), 2955–2968. https://doi.org/10.1016/S1352-2310(99)00089-8

Walsh, K. J., Milligan, M., Woodman, M., & Sherwell, J. (2008). Data mining to characterize ozone behavior in Baltimore and Washington, DC. *Atmospheric Environment*, *42*(18), 4280–4292. https://doi.org/10.1016/j.atmosenv.2008.01.012

Whitten, G. Z., Heo, G., Kimura, Y., McDonald-Buller, E., Allen, D. T., Carter, W. P. L., & Yarwood, G. (2010). A new condensed toluene mechanism for Carbon Bond: CB05-TU☆. *Atmospheric Environment*, *44*(40), 5346–5355. https://doi.org/10.1016/j.atmosenv.2009.12.029

Winer, A. M., Peters, J. W., Smith, J. P., & Pitts, J. N. (1974). Response of commercial chemiluminescent nitric oxide-nitrogen dioxide analyzers to other nitrogen-containing compounds. *Environmental Science & Technology*, *8*(13), 1118–1121. https://doi.org/10.1021/es60098a004

Wolfe, G. M., Marvin, M. R., Roberts, S. J., Travis, K. R., & Liao, J. (2016). The Framework for 0-D Atmospheric Modeling (F0AM) v3.1. *Geoscientific Model Development*, *9*(9), 3309–3319. https://doi.org/10.5194/gmd-9-3309-2016

Wolff, G. I. (1993). On A NO x -Focused Control Strategy to Reduce O 3. *Air & Waste*, *43*(12), 1593–1596. https://doi.org/10.1080/1073161X.1993.10467229

Yarwood, G., Gookyoung, H., Carter, W. P. L., & Whitten, G. Z. (2012). *Environmental Chamber Experiments to Evaluate NOx Sinks and Recycling in Atmospheric Chemical Mechanisms AQRP Project 10-042*. Retrieved from http://aqrp.ceer.utexas.edu/projectinfo%5C10-042%5C10-042 Final Report.pdf